

RESEARCH

GPER1 deficiency causes sex-specific dysregulation of hippocampal plasticity and cognitive function

Aune Koitmäe^{1,*}, Yannik Karsten^{1,2,*}, Xiaoyu Li^{1,3}, Fabio Morellini⁴, Gabriele M Rune⁵ and Roland A Bender¹ 

¹Institute of Neuroanatomy, University Medical Center Hamburg, Hamburg, Germany

²Department of Genetics and Molecular Biology, Institute of Biology, University of Magdeburg, Magdeburg, Germany

³Department of Endocrinology, Zhongda Hospital, School of Medicine, Southeast University, Jiangsu, China

⁴Research Group Behavioral Biology, Center for Molecular Neurobiology, Hamburg, Germany

⁵Institute of Cell Biology and Neurobiology, Universitätsmedizin Charité Berlin, Berlin, Germany

Correspondence should be addressed to R A Bender: r.bender@uke.de

(*A Koitmäe and Y Karsten contributed equally to this work)

Abstract

Estrogens regulate synaptic properties and influence hippocampus-related learning and memory via estrogen receptors, which include the G-protein-coupled estrogen receptor 1 (GPER1). Studying mice, in which the *GPER1* gene is dysfunctional (GPER1-KO), we here provide evidence for sex-specific roles of GPER1 in these processes. GPER1-KO males showed reduced anxiety in the elevated plus maze, whereas the fear response ('freezing') was specifically increased in GPER1-KO females in a contextual fear conditioning paradigm. In the Morris water maze, spatial learning and memory consolidation was impaired by GPER1 deficiency in both sexes. Notably, in the females, spatial learning deficits and the fear response were more pronounced if mice were in a stage of the estrous cycle, in which E2 serum levels are high (proestrus) or rising (diestrus). On the physiological level, excitability at Schaffer collateral synapses in CA1 increased in GPER1-deficient males and in proestrus/diestrus ('E2 high') females, concordant with an increased hippocampal expression of the AMPA-receptor subunit GluA1 in GPER1-KO males and females as compared to wildtype males. Further changes included an augmented early long-term potentiation (E-LTP) maintenance specifically in GPER1-KO females and an increased hippocampal expression of spinophilin in metestrus/estrus ('E2 low') GPER1-KO females. Our findings suggest modulatory and sex-specific functions of GPER1 in the hippocampal network, which reduce rather than increase neuronal excitability. Dysregulation of these functions may underlie sex-specific cognitive deficits or mood disorders.

Key Words

- ▶ steroid hormone
- ▶ hippocampus
- ▶ spatial learning
- ▶ fear conditioning
- ▶ LTP
- ▶ AMPA receptor

Journal of Endocrinology
(2023) 258, e220204

Introduction

Estrogens affect learning and memory via two ways of intracellular signaling: classical estrogen signaling involves cytosol-based receptors, which translocate to the nucleus

upon ligand activation and bind to specific estrogen response elements (EREs) in target genes to induce gene transcription, whereas non-classical signaling involves

receptors which activate intracellular signaling cascades capable of mediating structural changes in neurons on a more rapid time scale (Taxier *et al.* 2020). Among the putative estrogen receptors (ERs) that convey non-classical estrogen signaling, G-protein-coupled estrogen receptor 1 (GPER1; previously termed GPR30) has received considerable attention. GPER1 is a seven-transmembrane receptor that signals via G_{a/s} subunits, causing activation of a variety of signaling pathways (Srivastava & Evans 2013, Alexander *et al.* 2017, Hadjimarkou & Vasudevan 2018). It was first identified in breast tissue (Carmeci *et al.* 1997) but is also expressed in the brain, including the hippocampus (Funakoshi *et al.* 2006, Brailoiu *et al.* 2007, Matsuda *et al.* 2008, Hazell *et al.* 2009, Akama *et al.* 2013, Waters *et al.* 2015, Meseke *et al.* 2018, Wang *et al.* 2018, Llorente *et al.* 2020). In the hippocampus, robust GPER1 expression is observed in the apical dendritic layers of cornu ammonis 1 3 (CA1–CA3) (Akama *et al.* 2013, Waters *et al.* 2015, Meseke *et al.* 2018, Li *et al.* 2021), suggesting that GPER1 regulates neural transmission at hippocampal pathways that are pivotal in processes of learning and memory (Taxier *et al.* 2020).

This hypothesis has been supported in several rodent studies using selective GPER1 agonists (G1; (Bologa *et al.* 2006)) or antagonists (G15, G36; (Dennis *et al.* 2009, 2011)). Kim and colleagues (Kim *et al.* 2019) demonstrated an increase in the spine density in the CA1 stratum radiatum after G1 infusion into the dorsal hippocampus, which correlates with a G1-induced improvement of spatial memory (Kim *et al.* 2016), object recognition (Kim *et al.* 2016, 2019, Lymer *et al.* 2017), and social recognition (Lymer *et al.* 2017). Infusion of GPER1 antagonist G15, in contrast, impairs memory (Kim *et al.* 2016). Comparable findings were reported if G1 or G15 were applied systemically (Hammond *et al.* 2012, Hawley *et al.* 2014, Gabor *et al.* 2015). In addition, G1 application increased field EPSP amplitude (Lebesgue *et al.* 2009) or slope (Kumar *et al.* 2015) in extracellular recordings in CA1 and increased evoked EPSC amplitude in a subset of whole-cell recordings of CA1 pyramidal cells in females (Lebesgue *et al.* 2009, Smejkalova & Woolley 2010). However, while all these findings clearly indicate a role of GPER1 in hippocampus-related memory formation and neuronal plasticity, their interpretation is limited by the fact that GPER1 agonists and antagonists were applied exogenously. Thus, these results may not adequately mirror GPER1 functions, when the

receptor is exposed only to its endogenous ligands. Genetically modified animals that specifically lack GPER1 offer the opportunity to circumvent these limitations. In these animals, effects are likely to be more subtle than if agonists are applied exogenously but may, on the other side, provide a more realistic picture of the actual impact that the receptor has in the complex networks of the nervous system.

Here, we used a genetically modified mouse strain, in which the gene encoding for GPER1 was rendered dysfunctional by the insertion of a neomycin resistance cassette (Wang *et al.* 2008) for behavioral testing, electrophysiology, and expression analyses of synaptic proteins. In these mice, GPER1 deficiency affects the development of the thymus (Wang *et al.* 2008) and the regulation of blood pressure (Haas *et al.* 2009). Also, a tendency toward visceral obesity has been reported (Haas *et al.* 2009). But no major health impairment is evident, which may render the mice unsuitable for studies on cognitive functions. Moreover, GPER1-deficient (GPER1-KO) female mice have a regular estrous cycle and their reproductive capacity is not different from that of the corresponding wildtype (WT) mice (Wang *et al.* 2008, Otto *et al.* 2009). Thus, an impaired synthesis of sex hormones is unlikely to distort the results, and the mice offer the possibility to consider the female estrous cycle as a regulating factor for the functions of GPER1. Consequently, in our study, mice were not gonadectomized, as gonadectomy may also cause dysregulation of the hypothalamic–pituitary axis (Prange-Kiel *et al.* 2008). Thus, both males and females were examined to determine potential sex differences, which have been demonstrated in a variety of hippocampal functions that are influenced by sex hormones (Vierk *et al.* 2012, Tabatadze *et al.* 2015, Wang *et al.* 2018, Brandt *et al.* 2020), including functions which are regulated by GPER1 (Li *et al.* 2021). In addition, to account for the potential effects of the estrous cycle, the cycle stage of the females was determined and findings were correlated to cycle stages, in which serum levels of the most potent estrogen, 17 β -estradiol (E2), are rising or high (diestrus, proestrus='E2 high') or are declining or low (estrus, metestrus='E2 low') (Frick *et al.* 2015, Nilsson *et al.* 2015). Our results support previous assumptions of an influence of GPER1 on hippocampal learning processes but suggest that GPER1 functions in the hippocampal network are complex and involve regulatory mechanisms that are sex- and cycle stage specific.

Experimental procedures

Animals

GPER1-deficient B6.129S6-*Gper1tm1Cwan/J* mice (GPER1-KO) were obtained from Jackson Laboratories. In this mouse strain, the gene encoding for GPER1 (exon 3 on chromosome 5) was rendered dysfunctional by the insertion of a neomycin resistance (neo) cassette, as described previously by Wang *et al.* (2008). Mutants were introduced into the research animal facility of the University Medical Center Hamburg-Eppendorf (UKE) via embryo transfer. GPER1 heterozygotes (+/-) were subsequently used for breeding, and WT (+/+) and GPER-KO (-/-) littermates were used for experimental analyses (behavioral testing, electrophysiology, and synaptic protein analyses; see below).

Genotyping

To identify the genotype of the offspring, tail tip biopsies were collected and DNA was extracted using 'Extract-N-Amp Tissue PCR Kit' (Merck) according to the manufacturer's instructions. An aliquot of the extract was used for PCR amplification of the GPER1 sequence by adding 'Extract-N-Amp PCR reaction mix' (which contains: salts, dNTPs, and *Taq* polymerase), PCR-grade water, and specific primers (Eurofins Genomics):

WT/GPER1 forward: 5'-GAG CAC ATC TGA GGA GCA CTT TGC TGT CTC C-3'

WT/GPER1 reverse: 5'-GTG CCA CCA ACA CCC AGC TCA CAC AGC-3'

neo reverse: 5'-GGA TCT CAC ATC TGA GGA TCA CCT TGC TGT CTC C-3'

PCR was run with initial denaturation (94°C for 2 min) followed by a three-step denaturation-annealing-elongation cycle at 94°C for 30 s, 62°C for 30 s, and 68°C for 30 s for 35 cycles (Wang *et al.* 2008). PCR products were separated on a 1% agarose gel (stained with ethidium bromide) by electrophoresis, exposed to UV light and photographically captured.

In addition, to confirm GPER1 deficiency, total RNA was isolated from frontal lobe, cerebellar, and hippocampal tissue of mice which were identified as GPER1-KO or WT ($n=3$ each) by PCR genotyping (protocol as above), using the RNeasy kit (Qiagen). Subsequently, purified RNA was treated with DNase I to remove any potential genomic DNA and reverse transcriptase (RT)-PCR was executed using the Maxima First Strand cDNA

Synthesis Kit (Fisher Scientific). Priming of the RT reactions was performed using random hexamers, followed by amplification for GPER1 using the following primers:

Forward: 5'-ATG GAT GCG ACT ACT CCA GCC CAA ACT GTG G-3'

Reverse: 5'-TCA CAC AGC ACT GCT GAA CCT GAC CTC TGA CTG-3'

Estrous cycle staging

To determine the estrous cycle stage of the female mice, a vaginal swab was taken by inserting a phosphate-buffer-saline (PBS)-soaked cotton swab (ϕ 2 mm) into the vaginal canal. Smears were then spread onto microscopic slides and air-dried before staining was performed with crystal violet stain and analyzed according to McLean and colleagues (McLean *et al.* 2012), as this method offers a quick and reliable way to assess the stage of the estrous cycle on a daily basis.

Behavior analyses

A total of 37 GPER1-KO mice (26 females, 11 males) and 32 WT mice (20 females, 12 males) were used for behavioral testing. The animals were initially kept in open cages under standard conditions in the UKE research breeding facility. After reaching adulthood (postnatal day (P) 60–90), they were transferred to the experimental facility at the Center of Molecular Neurobiology Hamburg (ZMH), in which mice were kept under controlled conditions (21 \pm 2°C, 45% humidity, illumination: 19:30–7:30 h, food and water *ad libitum*). Male and female mice were kept in the same room, but in separate cages (type 2L), in groups of up to six females or two males per cage. At the end of the habituation phase, which lasted 2 weeks, the cycle stage of the females was determined ('staged') the first time, while 'sham handling' was performed with the male mice. Thus, the stress level caused by the handling procedure remained the same between sexes. Subsequently, each mouse underwent a schedule of behavioral tests (Supplementary Fig. 1, see section on supplementary materials given at the end of this article) that assessed exploration and anxiety behavior ('open field,' OF and 'elevated plus maze,' EPM), followed by tests for spatial learning capacity and memory consolidation ('Morris water maze,' MWM), and for 'contextual fear conditioning' (CFC). The testing phase lasted on average 60 days (ranging between 23 and 84 days, depending on the availability of the

testing facilities). Before OF and EPM testing, the females were cycle staged anew and the males sham-handled accordingly. For MWM, which lasted more than 1 day, the cycle stage of female mice was determined on the second day, at which memory was first tested by a probe trial ('short-term memory,' day 2), and females were categorized with the determined stage throughout the experiment. Similarly, for CFC, cycle staging was performed on day 2, at which 'recall' was examined. Female mice, for which cycle staging was ambiguous, were excluded from the analysis. All experiments were conducted during the dark cycle (from 9:00 h at the earliest to 18:00 h at the latest) in a room adjacent to the husbandry illuminated with dim red light.

In total, five cohorts of age-matched mice were tested, each comprising of 12–20 animals of both sexes and genotypes. The results of the individual cohorts were pooled for statistical analysis. Mice were tested during their dark phase and all experiments were conducted in accordance with the German and European Union laws on protection of experimental animals and were approved by the local authorities of the City of Hamburg, Germany (N19/059). Every effort was taken to minimize the number of animals used and to minimize their pain or discomfort.

Open field

The OF test was performed with naive animals and represented the first test in a sequence of behavioral tests. The experimental apparatus consisted of a 50 × 50 cm arena enclosed by 40 cm high walls, illuminated with white light (25 lux). Animals were taken from their home cage, gently placed in one corner of the arena and tested for 20 min. Mice were tracked on video for the entire duration of the test. Total distance moved, mean velocity, mean distance to the wall, number of entries to the center, and the time spent in the center (an imaginary inner square of 20 × 20 cm) were analyzed with the software EthoVision (Noldus, Wageningen, The Netherlands).

Elevated plus maze

The EPM arena had the shape of a plus with four 30 cm long and 5 cm wide arms, connected by a 5 × 5 cm center. Two opposing arms were bordered by 15 cm high walls (closed arms), whereas the other two arms (open arms) were bordered by a 2 mm rim. The maze was elevated 75 cm from the floor. Experiments were performed in total darkness and recorded using an infrared video camera. For a trial, a mouse was placed in the center facing an

open arm and left on the maze for 5 min. The following parameters were manually analyzed: number of entries into open and closed arms (counted when all four paws were on one arm), transitions from a closed arm into an open arm, time spent in open and in closed arms, and latency to enter open arms. *The Observer XT* software (Noldus, Wageningen, the Netherlands) was used for this purpose.

Morris water maze

For MWM testing, mice were first subjected to a pre-training protocol (Fellini *et al.* 2006), during which the animals were placed in a miniature water maze (Ø 30 cm) and had to locate the submerged platform. After pre-training, mice were trained and tested in a basin with a diameter of 145 cm. The water temperature was $20 \pm 1^\circ\text{C}$ and the water was made opaque by non-toxic white paint. A platform (Ø 14 cm) was placed ~1 cm below the water surface, invisible to the mice, so they had to rely on visual extra maze landmarks (different, contrasting black and white patterns) to locate it. The setting was occluded from the rest of the room by black curtains, and the set-up was illuminated by spotlights, which provided illumination of 100 lux on the surface of the water. For the learning and probe trials, mice were transported to the water maze in a plastic cup attached to a long stick. The opening of the cup was positioned toward the basin wall to allow the mouse to slide into the water while not being able to see the pool. The mice started from four symmetrical starting positions in a pseudo-randomized order and were given 90 s to swim in the pool and find the hidden platform. After 10 s on the platform, the mice were rescued and returned to their home cages to warm and dry under infrared light. If an animal did not find the platform within 90 s, the position of the platform was indicated by the experimenter. On day 1, mice underwent four learning trials with inter-trial intervals of 10–20 min. The distance moved before reaching the platform ('distance to platform') and the 'escape latency' (i.e. the time the mouse requires to find the platform) were determined in these trials. On day 2, two more learning trials were performed, followed by a probe trial ('short-term memory,' 20 min after the second learning trial), in which the platform was removed, and the mice had to swim for 60 s before being returned to their home cages. The time spent at the platform's former location ('time on platform location') and in the target quadrant ('time in quadrant') was used to probe the short-term memory capacity of the mice to locate the platform. In addition, the mean distance from the

platform's location ('mean distance to platform') was determined for each mouse. Day 2 was concluded by two learning trials. Day 3 began with another probe trial ('long-term memory,' 24 h after the last learning trial), which was followed by two learning trials. In addition, 'remote memory' (Albo & Gräff 2018) was tested with a final probe trial 1 week after day 3. All trials were video-recorded and analyzed with the video tracking system EthoVision (Noldus, Wageningen, the Netherlands). Trials that were not successfully recorded (short-term memory: 6 mice, long-term memory: 1 mouse) were excluded from the analysis.

Contextual fear conditioning

For CFC, mice were placed in a chamber (23.5 long × 23.5 wide × 19.5 cm high, illuminated by 15 lux) with Plexiglas walls and ceiling and a stainless-steel grid floor. The animals could explore the environment (*neutral stimulus*) for 2 min, then received three electric foot-shocks (each 340 µA for 1 s, with an inter-shock interval of 40 s) during the following 2 min (*conditioned stimulus*). On day 2, mice were analyzed for memory retrieval by exposing them to the same environment for 4 min, but without electrical shock. The memory of the environment triggered 'freezing' (defined as the absence of body movement for at least 1 s) as a defense reaction to the expected shock (Bolles 1970). This conditioned response (rel. time spent freezing) was analyzed by a modified version of the infrared sensor Mouse-E-Motion (Infra-e-motion, Hamburg, Germany). On day 3, mice were placed for 4 min in a different chamber (15 long × 25 wide × 25 cm high, made of white polypropene) to test for generalized fear.

Electrophysiology

Hippocampal slice preparation and extracellular recordings were performed according to Vierk and colleagues (Vierk *et al.* 2012). Briefly, mice (8–10 weeks old) were decapitated under deep isoflurane anesthesia in the morning (8–9:00 h). Immediately after decapitation, the brains were rapidly removed and transferred in an ice-cold, slushy high sucrose artificial cerebrospinal fluid (aCSF) containing (in mM) sucrose 212.7, KCl 2.6, NaHCO₃ 26, NaH₂PO₄ 1.23, MgSO₄ 7, glucose 10, and CaCl₂ 1, pH 7.4. Acute transverse slices (400 µm) were then sectioned with a vibratome (Leica VT1200) and transferred to a brain slice holding chamber filled with aCSF (in mM): NaCl 119, KCl 2.5, NaHCO₃ 26, NaH₂PO₄ 1.25, MgSO₄ 1.3, glucose 10, CaCl₂ 2.5, and pH 7.4.

For the first 30 min, slices were incubated at 30°C, thereafter for recovery at room temperature (RT) for at least 1.5 h before starting the recordings. The slices were constantly equilibrated with 95% O₂ and 5% CO₂ to keep physiological conditions stable.

The recording chamber was perfused with constantly carboxygenated and equilibrated aCSF (2.5 mL/min). For recordings, a fine stimulating borosilicate glass microelectrode was filled with aCSF and used to stimulate Schaffer collaterals in CA3 stratum radiatum. The resistance of the stimulating electrode was around 1 MΩ. The recording electrode, also filled with aCSF, had a resistance of ~3 MΩ and was localized to the CA1 dendrites in the middle of stratum radiatum. Field excitatory postsynaptic potential (fEPSPs) initial slopes (mV/ms) were measured and presented relative to baseline (%). Recordings were performed at constant temperature (28°C). The temperature was controlled in the recording chamber using a temperature controller (npi MTC-20/2SD).

Input-output curve

To determine the influence of genotype on basal synaptic transmission, input-output (I/O) curves were recorded using the software Clampex (version 10.4). To evaluate the maximum amplitude of the synaptic response within a window, software Clampfit (version 10.4) was used. Test pulses were applied, starting from 5 V up to saturation, and fEPSP slopes were plotted as a function of stimulus strength. Following collection of I/O data, the stimulation intensity was set to obtain the half-maximal amplitude and stimulus pulse pairs were delivered (50 ms interpulse intervals).

G1 wash-in

In a subset of slices from WT (in total $n = 13$ from seven mice; three male, four female) and GPER1-KO mice ($n = 12$ from six mice; two male, four female), effects of G1 were determined. For that purpose, G1 (40 nM) was added to the aCSF after a stable (at least 10 min) fEPSP-baseline was established in the slice. Schaffer collateral-evoked fEPSPs were recorded 20 min after G1 wash-in was started.

Paired-pulse ratio

Paired-pulse facilitation was examined by delivering two consecutive stimuli with interstimulus intervals of 5, 10, 20, 50, 100, 200, or 500 ms. The paired-pulse ratio (PPR) was calculated as the ratio of the slope of the second fEPSP relative to the first.

Long-term potentiation

To perform long-term potentiation (LTP) experiments, the fEPSP slope was adjusted to 50% of the maximum slope. After a 10–20 min stable baseline recording, theta burst stimulation (TBS; 10 bursts of 4 pulses at 100 Hz; 200 ms between bursts) was induced. Synaptic transmission was monitored every 30 s and data were digitized at 10 kHz. After TBS, monitoring was continued for 40 min. To determine the magnitude of LTP induction, fEPSP slopes (% baseline) were averaged during the first 5 min of post-TBS recording (level 1), whereas fEPSP slopes from 30 min to 35 min post-TBS (level 2) were used to measure early LTP (E-LTP) maintenance.

Synaptic protein analysis

For Western Blot analyses of synaptic proteins, hippocampi of 50 adult (2–3 months old) naive mice (i.e., not subjected to behavior tests) were used (males: 12 WT, 14 KO; females: 13 WT, 11 KO). Mice were deeply anesthetized by CO₂ and decapitated (female mice were cycle staged before decapitation). Brains were then quickly removed and hippocampi were dissected, and quick-frozen in liquid nitrogen. For processing, deep-frozen hippocampi were thawed and tissue was homogenized in ice-cold RIPA lysis buffer (150 mM NaCl, 50 mM Tris (pH 7.5), 1% NP40, 0.1% SDS, 0.5% Na-deoxycholate, 5 mM EDTA, and a mixture of protease inhibitors). Lysates were cleared by centrifugation at 4°C and 13,000 **g** for 30 min. From each sample, 30–50 µg were diluted in water and 5× Laemmli buffer (62.5 mM Tris (pH 6.8), 2% SDS, 10% glycerol, 5% 2-mercaptoethanol, and 0.001% bromophenol blue) to a final volume of 12.5 µL. The samples were heated to 95°C for 5 min and then immediately cooled on ice. Subsequently, samples were loaded to a 10% polyacrylamide gel, separated by gel electrophoresis (Invitrogen) in Laemmli running buffer (10% SDS, 3% Tris, and 14% glycine) and then transferred electrophoretically to polyvinylidene fluoride membranes with transfer buffer (0.02% SDS, 0.015% Tris, 0.08% glycine). Each blot contained samples from WT and KO mice equally, but male and female tissue was run on different gels. For blotting, the membranes were blocked with either 5% bovine serum albumin (GluA1, GluN1, synaptophysin, spinophilin, synaptosomal nerve-associated protein 25 (SNAP25)) or with 5% milk powder (PSD95) in PBS at RT for 1 h and subsequently incubated with primary antibodies: rabbit anti-GluA1 (1:3000; Cell Signaling, Cat# 13185, RRID: AB_2732897), mouse anti-GluN1 (1:500; Millipore, Cat# MAB363,

RRID: AB_94946), mouse anti-PSD95 (1:2000; Sigma, Cat# P-246; RRID: AB_260911), rabbit anti-SNAP25 (1:1000; Abcam, Cat# AB41455; RRID: AB_945552), rabbit anti-spinophilin (1:1000; Millipore, Cat# 06-852, RRID: AB_310266), and mouse anti-synaptophysin (1:1000; Millipore, Cat# MAB5258; RRID: AB_2313839). In addition, mouse anti-GAPDH (1:10,000; Ambion, Cat# AM4300, RRID: AB_437392) or mouse anti-α-tubulin (1:10,000; Sigma, Cat# T6074, RRID: AB_477582) were applied for loading control. Secondary antibodies conjugated with horseradish peroxidase (1:2500; Jackson ImmunoResearch: goat anti-mouse-IgG and donkey anti-rabbit-IgG, Cat# 115035174 and 211032171, respectively; RRIDs: AB_2338512 and 2339149, respectively) were applied for 1 h at RT. The immunoreaction was visualized by enhanced chemiluminescence (FUSION-SL4 advanced imaging system; Vilber Lourmat Labtech, Eberhardzell, Germany).

Statistical analyses

For statistical analysis, Prism software (GraphPad 6) was used. Levels of significance were two-tailed and set to *P < 0.05, **P < 0.01, or ***P < 0.001. Kolmogorov-Smirnov test was used to determine whether data were normally distributed or not. An overview over all statistical results is provided in the 'Supplementary Table 1.' Selected results are presented within the figure legends or in the text to support the main findings. Quantitative data are presented as mean ± standard error of the mean (S.E.M.) within the text or graphically using bar graphs or box-and-whisker plots (minimum–maximum, including all data points), whenever applicable.

Behavior

Data were statistically analyzed using two-way analysis of variance (ANOVA) defining 'Sex' and 'Genotype' resp. 'Cycle stage' and 'Genotype' (OF, EPM, CFC), 'Genotype' and 'Trial (time)' (MWM – learning trials), or 'Sex × Genotype' and 'Time' resp. 'Cycle stage × Genotype' and 'Time' (MWM – probe trials) as between or within groups factors. Behavioral parameters served as dependent variables. *Post hoc* analyses were performed with uncorrected Fisher's LSD.

Electrophysiology

Except for G1 wash-in and LTP (within-slice development from level 1 to level 2), all data were analyzed using two-way ANOVA followed by *post hoc* tests (uncorrected Fisher's LSD). 'Sex' and 'Genotype' resp. 'Cycle stage'

and 'Genotype' were determined as fixed factors, and experimental parameters (fEPSP slope) as dependent variable. G1 wash-in data (GPER1-KO versus WT, without considering sex) were analyzed using the Mann-Whitney *U* test, as data distribution did not pass the normality test. For LTP, within-slice development of fEPSP slope from level 1 (L1, 0–5 min) to level 2 (L2, 30–35 min) was analyzed using paired *t*-test (if data were normally distributed) or Wilcoxon matched pairs signed rank test (= 'Wilcoxon,' if data were not normally distributed). Additionally, the differences between both levels (L2 and L1) were compared between experimental groups using two-way ANOVA (as above).

Western blot

Densitometric analyses of band intensities were performed using NIH Image J software. Target protein values were normalized to GAPDH (GluA1, GluN1) or α -tubulin (PSD96, SNAP25, spinophilin, synaptophysin) and are presented as %GAPDH resp. % α -tubulin. Data were statistically analyzed using two-way ANOVA with 'Sex' and 'Genotype' resp. 'Cycle stage' and 'Genotype' as fixed factors and relative protein expression as dependent variable. *Post hoc* analyses were performed using uncorrected Fisher's LSD.

Results

Confirmation of GPER1 deficiency

To control for the absence of GPER1 mRNA in the GPER1-KO mice, total mRNA was isolated from hippocampal, cerebellar, and frontal lobe tissue of mice, which were identified as either GPER1-KO or WT by PCR-genotyping ($n = 3$ each). GPER1 mRNA was reversely transcribed and quantified as described by Wang and colleagues (Wang *et al.* (2008); see also 'Experimental procedures'). In WT mice, all tested tissues yielded an amplicon of ~1200 bp, which spans the entire coding sequence within the mRNA for GPER1. In contrast, no signal was detectable in the presumed GPER1-KOs, confirming that GPER1 transcription was successfully eliminated in these mice (Supplementary Fig. 2).

Testing anxiety and locomotion

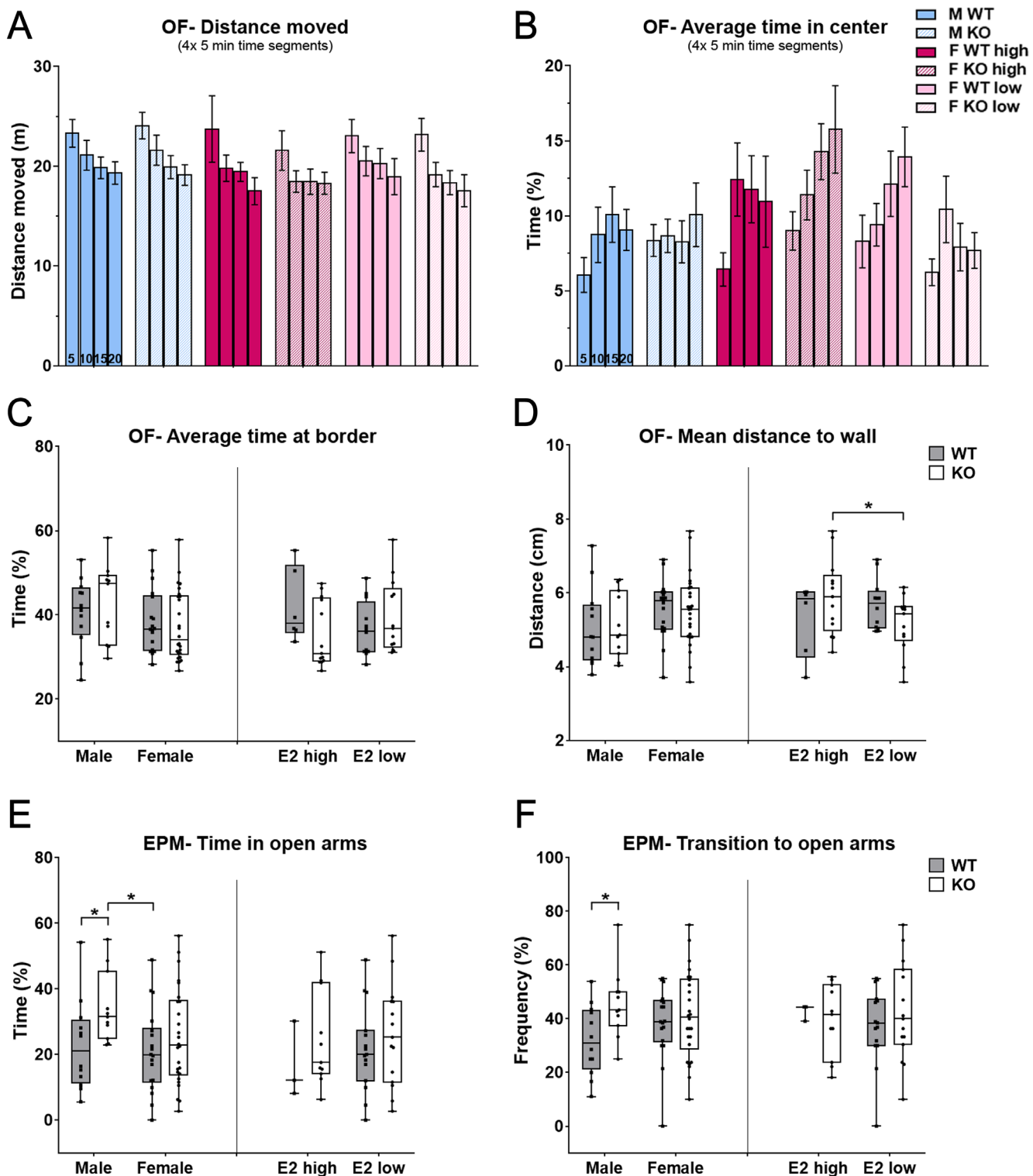
In the first set of behavior experiments, general locomotion and anxiety were examined using the OF and the EPM experimental paradigms. In the OF, GPER1-KO,

and WT mice showed comparable locomotion and none of them had to be excluded from the experiment. Experimental groups also showed comparable habituation, as all mice reduced the distance covered within the first 5 min interval in the subsequent intervals (Fig. 1A) and increased the time spent in the center of the arena (Fig. 1B). If the mean distance to the walls of the arena (Fig. 1C) and the relative time (% of total) spent in its periphery (Fig. 1D) were analyzed in the OF, no effect of genotype or sex was evident. The cycle stage, however, may have had an impact on behavior among the GPER1-KO females, as 'E2 low' females tended to stay closer to the wall than 'E2 high' females (Fig. 1D). No such effect was observed among the WT females. In contrast, for the EPM, two-way ANOVA indicated an effect of genotype, which was mainly elicited by the GPER1-KO males, as they spent significantly more time in open arms than both the WT males and females (Fig. 1E) and visited open arms significantly more often than the WT males (Fig. 1F), suggesting reduced anxiety specifically among the GPER1-KO males. No such differences were detected among the females, irrespective of cycle stage (Fig. 1E and F). Further, neither genotype nor sex significantly influenced the number of total transitions (WT male: 14.8 ± 1.6 , KO male: 16.6 ± 2.0 , WT female: 14.7 ± 1.0 , KO female: 14.4 ± 0.9) and the latency to enter open arms in the EPM (WT male: 27.5 ± 11.5 s, KO male: 16.3 ± 3.7 s, WT female: 39.0 ± 15.1 s, KO female: 26.4 ± 9.7 s). Self grooming, rearing, or the number of feces dropped were not different between the experimental groups (data not shown).

GPER1 deficiency impairs spatial learning and memory consolidation

A Morris water maze (MWM) was used to examine the spatial learning capacity of GPER1-KO mice. Before the learning trials, all mice underwent a pre-training protocol, which familiarized them with the aversive stimulus of the water. All mice swam well during this test phase and could be included in the analysis.

During the learning trials, mice successively reduced the swimming distance before reaching the platform without notable differences between genotypes, sexes, or cycle stages (Fig. 2A, B, C, and D). Similarly, if the time to reach the platform ('escape latency') was considered, all experimental groups learned equally well during the first day. However, in the first trial on the second day, GPER1-KO mice were comparatively disoriented and needed more time than the WTs to reach the platform,

**Figure 1**

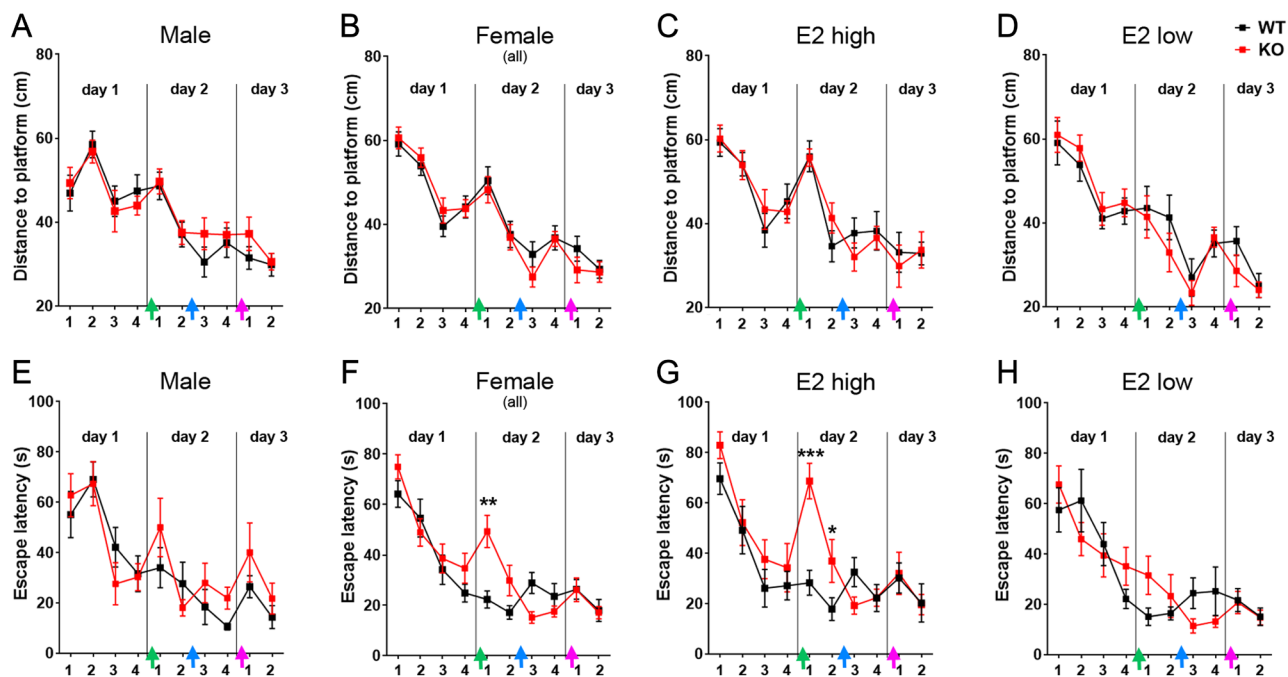
Reduced anxiety of GPER1-KO males in the 'Elevated Plus Maze.' (A, B) Graphs illustrate comparable habituation of tested mice, irrespective of genotype, sex and cycle stage, in the 'open field' (OF) paradigm, in which all mice successively reduced the distance they moved (A) and proportionally increased the time they spent in the center (B) during the 20-min testing period (divided into 4 × 5-min time segments). (C, D) No significant differences between genotypes or sexes were observed in the OF, if the average time spent at the border (C) and the mean distance to walls (D) was determined during the 20-min testing period. However, analysis of cycle stage effects indicated a higher tendency of 'E2 low' compared to 'E2 high' GPER1-KO females to stay

Figure 1 (Continued)

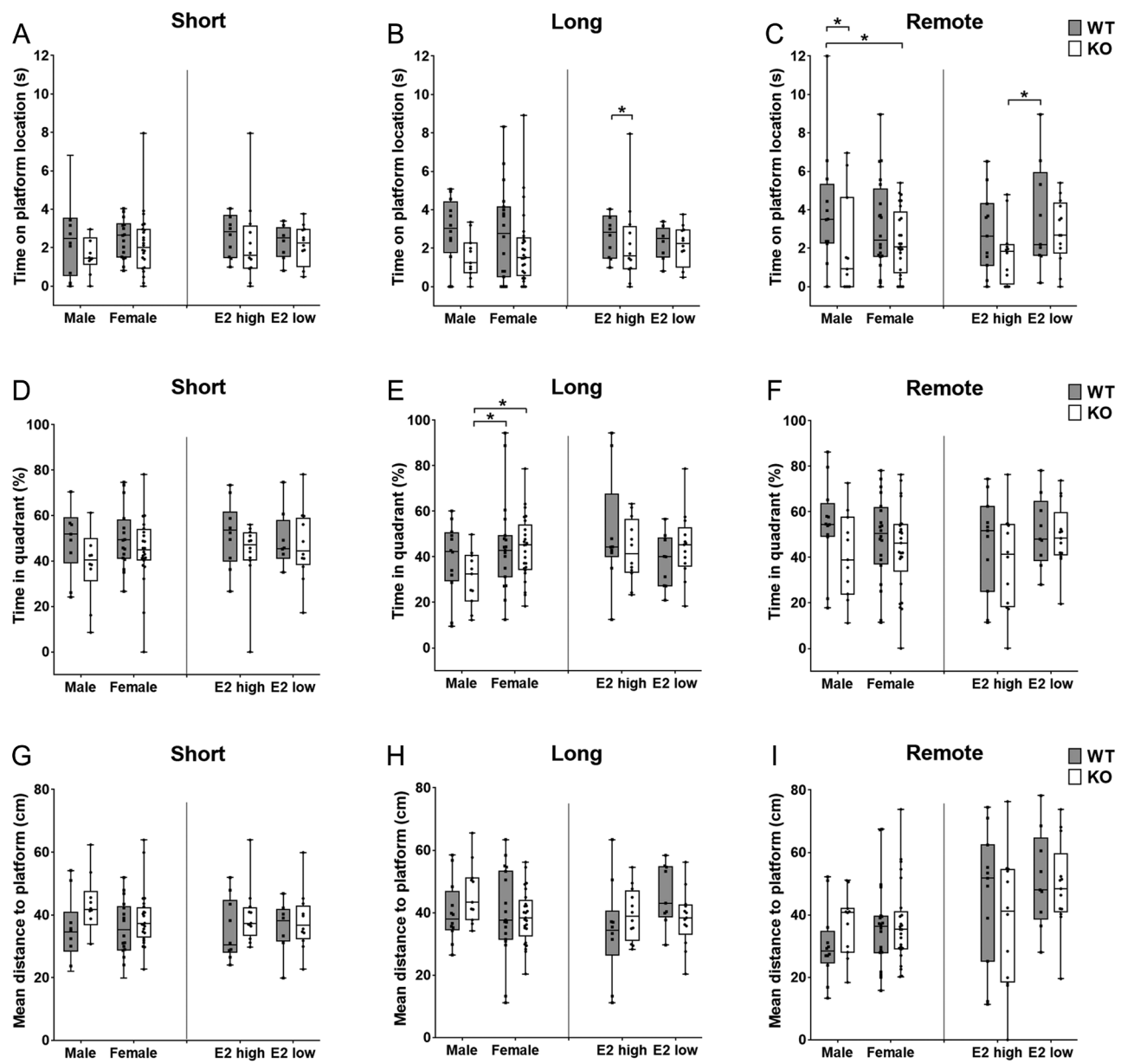
closer to the wall, indicative of increased anxiety (two-way ANOVA (interaction cycle \times sex): $F(1.40) = 4.2, P = 0.047$; KO E2 high: $5.9 \pm 0.3 (n = 13)$ versus KO E2 low: $5.1 \pm 0.2 \text{ cm} (n = 13)$ distance to wall, $P = 0.03$). No such difference was observed among the WT females (WT E2 high: $5.3 \pm 0.4 (n = 6)$ versus WT E2 low: $5.7 \pm 0.2 \text{ cm}$ mean distance ($n = 12$), $P = 0.4$). (E, F) For the 'Elevated Plus Maze' (EPM), grouped analyses indicated an effect of genotype for both the time spent in an open arm (E; two-way ANOVA (genotype): $F(1.63) = 5.2, P = 0.03$) and the transition to an open arm (F; two-way ANOVA (genotype): $F(1.63) = 4.7, P = 0.03$), while *post hoc* analyses suggested that this effect was mainly due to a different behavior of the GPER1-KO males. Specifically, GPER1-KO males spent significantly more time than WT males and females in an open arm (E; KO male: $34 \pm 3\% (n = 11)$ versus WT male: $23 \pm 4\% (n = 12)$, $P = 0.04$; versus WT female: $21 \pm 3\% (n = 18)$, $P = 0.01$; but versus KO female: $25 \pm 3\% (n = 26)$, $P = 0.07$) and entered open arms more frequently than WT males (F; KO male: $46 \pm 4\% (n = 11)$ versus WT male: $32 \pm 4\% (n = 12)$, $P = 0.03$), while no differences were detected among the females, irrespective of cycle stage. Quantitative data in the text and in A and B represent mean \pm S.E.M. Graphs in C, D, and F show box-and-whisker-plots (minimum–maximum) including all data points. Statistical details, which are not provided here, are available in the 'Supplementary Table 1.' Note that from the 32 WT (20 females, 12 males) and 37 GPER1-KO mice (26 females, 11 males), which underwent OF and EPM testing, two WT females had to be excluded from each analysis due to unclear cycle staging results (resulting in a total of 18 WT females). Further note that some females have switched from a 'E2 high' to a 'E2 low' cycle stage between OT and EPM, resulting in lower animal numbers for E2 high females in the EPM (WT: E2 high $n = 3$, E2 low $n = 15$; GPER1-KO: E2 high $n = 11$, E2 low $n = 15$). F = female; M = male. Numbers denote time segments: 0–5 (5), 5–10 (10), 10–15 (15), and 15–20 (20) minutes of observation.

suggesting that overnight consolidation of learning could have been hampered (Fig. 2E, F, G, and H). This effect was particularly evident among the females (Fig. 2F) and was most pronounced in those which were determined to be in an 'E2 high' cycle stage (Fig. 2G).

Probe trials were conducted in the same way as the learning trials, except that the platform was removed and the mice were left in the maze for a fixed duration of 60 s. Subsequently, the time spent at the location of the platform (Fig. 3A, B, and C), the time spent in the target

**Figure 2**

Impaired learning of GPER1-KO females in Morris Water Maze (MWM) learning trials. During the MWM learning trials, mice of both genotypes successively reduced the distance they swam ('distance to platform,' (A-D); two-way ANOVA (time): $P < 0.001$ for all experimental groups) and the time they needed to reach the platform ('escape latency,' (E-H); two-way ANOVA (time)) $P < 0.001$ for all experimental groups). However, the process of learning was less continuous among the GPER1-KO mice. Particularly, in the first learning trial of day 2, an effect was evident, as GPER1-KO mice needed significantly more time than WTs to reach the platform (E, F; two-way ANOVA, comparing results of trial 1 on day 2 (genotype): $F(1.64) = 8.6, P = 0.005$). This effect was mainly due to differences among the females (KO female: $49.4 \pm 6.4 \text{ s} (n = 25)$ versus WT female: $22.4 \pm 3.3 \text{ s} (n = 20)$, $P = 0.002$; F) and was most pronounced among 'E2 high' GPER1-KO females, which had a significantly higher escape latency compared to all other female experimental groups (G, H; two-way ANOVA, comparing results of trial 1 on day 2 (cycle): $F(1.41) = 14.9, P < 0.001$; (genotype): $F(1.41) = 19.0, P < 0.001$; KO E2 high: $68.7 \pm 7.1 \text{ s} (n = 12)$ versus WT E2 high: $28.5 \pm 5.0 \text{ s} (n = 11)$, $P < 0.001$; versus WT E2 low: $15.1 \pm 3.4 \text{ s} (n = 9)$, $P < 0.001$; versus KO E2 low: $31.5 \pm 7.6 \text{ s} (n = 13)$, $P = 0.001$; no significant difference was detected, if WT and KO E2 low females were compared, $P = 0.09$). Quantitative data represent mean \pm S.E.M. Further statistical details are available in the 'Supplementary Table 1.' Numbers on the x-axis indicate the number of the learning trial performed at the particular day. Green arrows denote the time of cycle staging (resp. pseudo-staging for the males), blue arrows indicate the probe trials for 'short-term memory' (day 2), and pink arrows those for 'long-term memory' (day 3). Note that 1 GPER1-KO female had to be excluded due to unclear cycle staging results, resulting in a total of 25 KO females and 20 WT females for MWM analyses.

**Figure 3**

Impaired spatial memory of GPER1-KO mice in Morris water maze (MWM) probe trials. MWM probe trials were performed during day 2 ('short'-term memory; A, D, G), on the morning of day 3 ('long'-term memory; B, E, H), and 1 week after the last learning trial ('remote' memory; C, F, I). The time the mice swam at the position of the platform ('Time on platform location'; A-C) or in the target quadrant ('Time in quadrant'; D-F), and the mean distance the mice kept from the platform ('Mean distance to platform'; G-I) were analyzed as parameters for spatial learning and memory. Further, the progress the mice made from the first to the last probe trial (ANOVA fixed factor: 'Time') was considered in the statistical analyses. These revealed an effect of sex × genotype for 'Time on platform location' (two-way ANOVA (sex × genotype): $F(3,185) = 3.8, P = 0.01$) and 'Time in quadrant' (two-way ANOVA (sex × genotype): $F(3,185) = 3.4, P = 0.02$). Post hoc analyses revealed deficiencies specifically of GPER1-KO males in the remote ('Time on platform location,' C; KO male: 2.0 ± 0.8 s ($n = 11$) versus WT male: 4.0 ± 0.9 s ($n = 12$), $P = 0.02$) and in the long-term memory trials ('Time in quadrant,' E; KO male: $30 \pm 4\%$ ($n = 11$) versus WT female: $45 \pm 5\%$ ($n = 19$), $P = 0.02$; versus KO female: $44 \pm 3\%$ ($n = 25$), $P = 0.03$; but versus WT male: $39 \pm 5\%$ ($n = 12$), $P = 0.24$). GPER1-KO females also performed poorly ('Time on platform location' (remote), C; KO female: 2.3 ± 0.3 s ($n = 25$) versus WT male: 4.0 ± 0.9 s ($n = 12$), $P = 0.02$; but versus WT female: 3.2 ± 0.5 s ($n = 20$), $P = 0.16$), but analyses considering the cycle stage suggested that it were mainly the GPER1-KO females, which were in an 'E2 high' cycle stage on the day before (see Fig. 2), which had difficulties to locate the platform in the long-term (B; KO E2 high: 1.7 ± 0.4 s ($n = 12$) versus WT E2 high: 3.4 ± 0.8 s ($n = 10$), $P = 0.046$) and remote memory trials (C; KO E2 high: 1.7 ± 0.5 s ($n = 12$) versus WT E2 low: 3.6 ± 0.9 s ($n = 9$), $P = 0.03$; versus WT E2 high: 2.8 ± 0.6 s ($n = 11$), $P = 0.17$). Progress over time was observed for parameters 'Time in quadrant' (two-way ANOVA (time): $F(2,185) = 3.4, P = 0.04$) and 'Mean distance to platform' (two-way ANOVA (time): $F(2,185) = 4.6, P = 0.01$). However, only male mice ('Time in quadrant,' WT male: $39 \pm 5\%$ (long-term) versus $54 \pm 5\%$ (remote, $n = 12$), $P = 0.03$; 'Mean distance to platform,' WT male: 40 ± 3 cm (long-term) versus 30 ± 3 cm (remote, $n = 12$), $P = 0.03$; 'Mean distance to platform,' KO male: 46 ± 3 cm (long-term) versus 37 ± 3 cm (remote, $n = 11$), $P = 0.049$) but not the females

Figure 3 (Continued)

(see data in Supplementary Table 1) improved their performance significantly. No effect of genotype was noted in this analysis. Quantitative data in the text represent mean \pm s.e.m. Graphs show box-and-whisker-plots (minimum–maximum) including all data points. Note that six mice (two WT female, one KO female, two WT male, one KO male) had to be excluded from the analysis of short-term memory and one WT female from the analysis of long-term memory due to technical problems with the Ethovision system, resulting in a total of 62 mice (18 WT female/24 KO female/10 WT male/10 KO male) for short-term, of 67 mice (19/25/12/11) for long-term and of 68 mice (20/25/12/11) for remote memory analysis. One female mouse was excluded from all analyses due to unclear cycle staging (see Fig. 2).

quadrant (Fig. 3D, E, and F), and the mean distance to the platform (Fig. 3G, H, and I) were determined. Probe trials were conducted during day 2 (following upon two learning trials to determine 'short-term memory'), on the morning of day 3 ('long-term memory'), and 1 week after day 3 ('remote memory'). It was noted that GPER1-KO mice performed poorer than the WT mice, as they spent generally less time compared to WT mice at the platform's location and in the target quadrant in the long-term (Fig. 3B and E) and remote memory tests (Fig. 3C and F), whereas no differences were apparent, if short-term memory was examined (Fig. 3A and D). Notably, among the females, the GPER1-KOs, which had been determined to be in an 'E2 high' cycle stage the day before (day 2), had more difficulties than 'E2 high' WT females to locate the platform in the long term, but not the short-term, probe trial (Fig. 3B). This observation is in line with the impairment seen during learning (Fig. 2) suggesting that 'E2 high' GPER1-KO females have some deficits in consolidating and/or retrieving memories. In addition, both male and female GPER1-KO mice had greater problems than WT mice to find the platform in the remote memory tests (Fig. 3C). Again, among the GPER1-KO females, those which were in an 'E2 high' cycle stage on day 2 had the poorest performance (Fig. 3C). Thus, altogether the data indicate that GPER1 deficiency affects the consolidation and/or retrieval of spatial memories, an effect that seems to become more pronounced as memories get older. Further of note: if the progress over time was considered, a sex difference was observed, as male, but not female, mice improved their performances in remote compared to long-term memory tests (Supplementary Table 1). However, as this was observed for both the GPER1-KO and the WT males, it is unlikely to be a genotype effect.

Testing for contextual fear conditioning

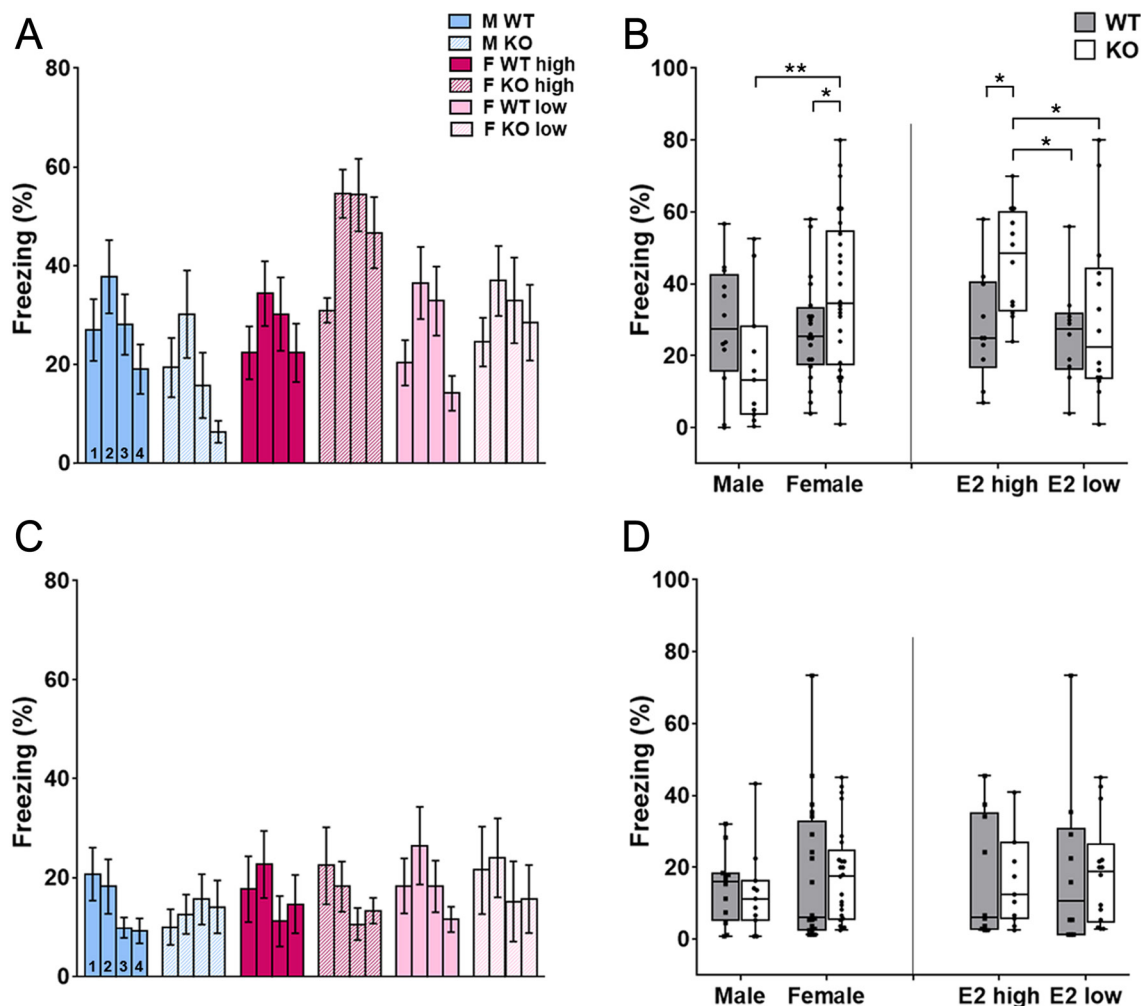
GPER1 functions have previously been suggested in networks which govern fear and anxiety, including the amygdala (Kastenberger *et al.* 2012, Tian *et al.* 2013, Kastenberger & Schwarzer, 2014, Hart *et al.* 2014). Therefore, we next examined the capacity of GPER1-KO

mice to develop contextual fear conditioning (CFC), which requires both hippocampal and amygdalar activity (Izquierdo *et al.* 2016). Mice were initially fear conditioned by receiving unsigned foot shocks while in the conditioning chamber (day 1). On day 2, mice were re-introduced into the conditional chamber and observed for 4 min without applying a foot shock. Within the chamber, mice showed a freezing response that was strongest during the second minute and decreased thereafter (Fig. 4A). However, while this temporal sequence was generally similar in all experimental groups (Fig. 4A), we noticed that GPER1-KO females adapted less well to the situation and spent in total a significantly higher proportion of time freezing compared to WT females and to GPER1-KO males (Fig. 4B). Analysis of cycle stage effects revealed that this mainly involves the 'E2 high' GPER1-KO females, which showed significantly increased freezing, if compared to all other female experimental groups (Fig. 4B).

On day 3, generalized fear was tested by placing the animals in a chamber different from the conditioned context. In this environment, mice generally showed less freezing than the day before, indicating that they discriminated against the conditioned context (Fig. 4C). No differences between the genotypes, sexes, or cycle stages were observed on day 3 (Fig. 4D).

Altered synaptic properties in hippocampal CA1 of GPER1-deficient mice

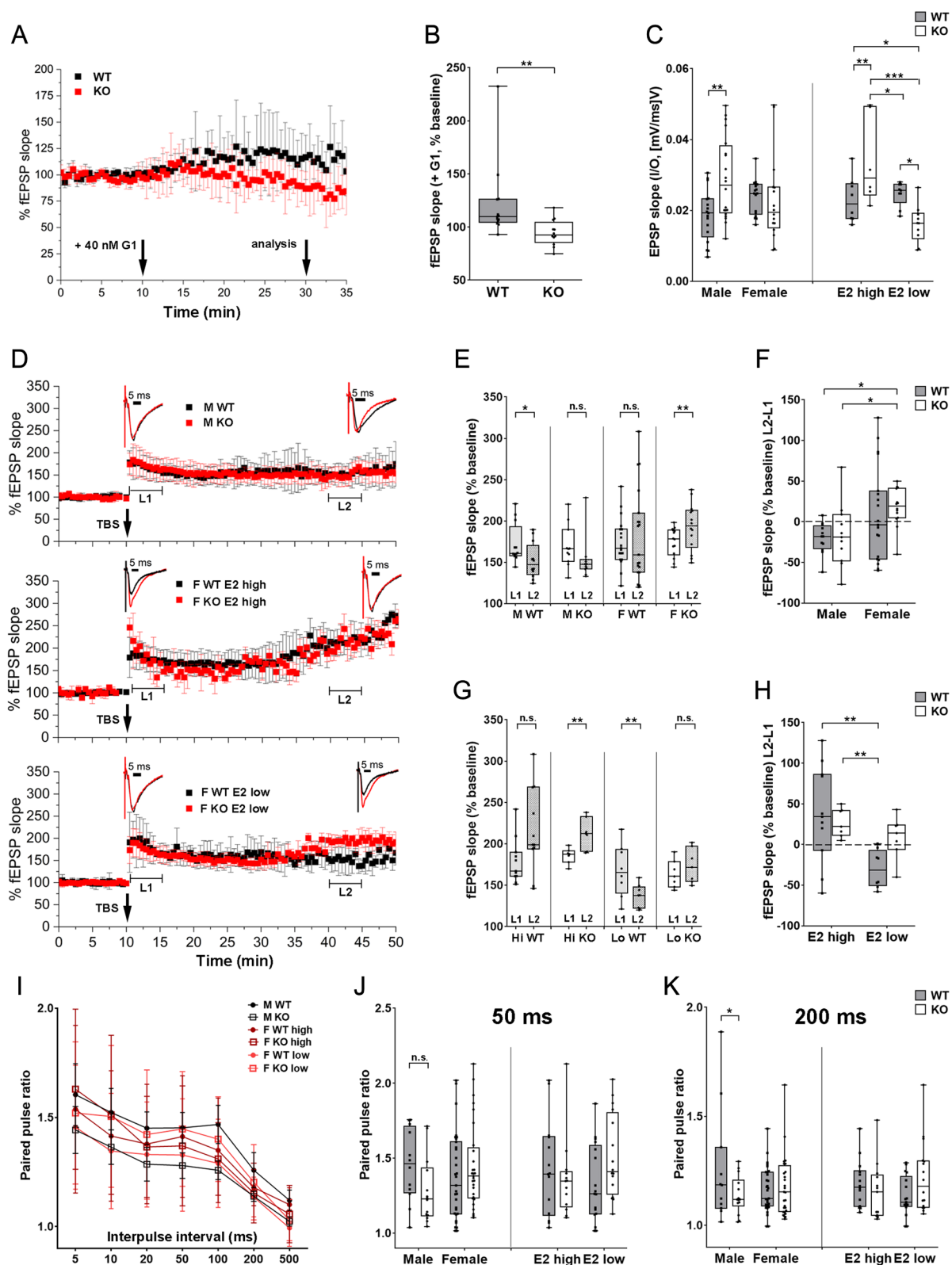
Behavior analyses (above) indicate that GPER1-deficiency impacts the mice' behavior with respect to spatial learning and context-related fear memory. We therefore examined next how GPER1-deficiency affects the synaptic transmission at the Schaffer collateral synapses in CA1, which is crucial for spatial learning (Martin & Clark 2007). For this purpose, we performed extracellular recordings in CA1 and determined excitatory field potentials (fEPSPs) that resulted from stimulating the Schaffer collateral pathway in CA3. In the first set of experiments, we washed-in GPER1 agonist G1 to acute hippocampal slices and observed that G1, as shown before (Lebesgue *et al.* 2009, Kumar *et al.* 2015),

**Figure 4**

Enhanced fear response in 'E2 high' GPER1-KO females. (A, B) Behavior testing was completed by contextual fear conditioning (CFC). In this paradigm, electrical footshocks, applied in an optically cued chamber (day 1), resulted in a marked fear response ('freezing') if the mice were placed in the same chamber on the next day (day 2). This response was strongest in the second (of four) minutes within the chamber and decayed thereafter. While this temporal sequence was similar in all experimental groups (A), analysis of the proportion spent in 'freezing' during the total 4-min period (B) indicated an effect of interaction sex \times genotype (two-way ANOVA (interaction): $F(1.65) = 5.0, P = 0.03$) and an effect of sex (two-way ANOVA (sex): $F(1.65) = 4.1, P = 0.047$) that was largely due to the GPER1-KO females, which adapted less well and spent on average a significantly larger proportion of the 4-min period in the 'freezing' state compared to WT females and GPER1-KO males (B; KO female: $38 \pm 4\% (n = 26)$ versus WT female: $27 \pm 3\% (n = 20), P = 0.049$; versus KO male: $18 \pm 5\% (n = 11), P = 0.004$; but versus WT male: $28 \pm 5\% (n = 12), P = 0.13$). Subsequent analysis of cycle influence revealed an effect of genotype (two-way ANOVA (genotype): $F(1.42) = 4.6, P = 0.04$) that was due to the 'E2 high' GPER1-KO females, which showed significantly enhanced freezing compared to all other female experimental groups (B; KO E2 high: $46 \pm 4\% (n = 12)$ versus WT E2 high: $28 \pm 5\% (n = 10), P = 0.02$; versus WT E2 low: $26 \pm 4\% (n = 10), P = 0.01$; versus KO E2 low: $31 \pm 6\% (n = 14), P = 0.03$). C, D) On the next day (day 3), placement of the mice into a new chamber to test for generalized fear resulted in reduced freezing compared to day 2, indicating context discrimination (C). No significant differences between genotypes, sexes, or cycle stages were observed under these conditions (D). Quantitative data in the text and in A and C represent mean \pm S.E.M. Statistical details, which are not provided here, are available in the 'Supplementary Table 1.' Graphs in B and D show box-and-whisker-plots (minimum-maximum) including all data points. F = female; M = male. Numbers denote time segments: first, second, third, and fourth minute of observation.

caused a significant increase of the fEPSP slope in slices from WT mice ($122 \pm 10\%$ rel. to baseline) but not in those from GPER1-KOs ($95 \pm 4\%$), confirming that these do not contain functional GPER1 (Fig. 5A and B). We next established I/O curves and noticed that the fEPSP slope in relation to stimulus intensity was significantly steeper in slices from GPER1-KO males compared to

those from WT males, suggesting that the CA1 network is more excitable in GPER1-KO males (Fig. 5C). I/O differences were also observed among the females, but these depended on the cycle stage. Thus, as for the males, I/O slopes were significantly steeper in slices from GPER1-KO compared to WT, if the slices were derived from 'E2 high' females (Fig. 5C). In contrast, if the slices

**Figure 5**

Synaptic properties are sex-specifically altered in CA1 of GPER1-KO mice. (A) Extracellular field potential (fEPSP) recordings at Schaffer collateral synapses in CA1 show that G1 supplementation (40 nM, first arrow) to the aCSF increases the fEPSP slope in slices from wildtype (WT) mice after 20 min (second arrow) but not in those from GPER1-KO mice, demonstrating that GPER1 signaling is abolished in the GPER1-KOs. (B) Quantitative analysis of the fEPSP

Figure 5 (Continued)

slopes 20 min after G1 exposure (second arrow in A): WT + G1: $122 \pm 10\%$ rel. baseline ($n = 13$ slices/7 mice; 3 male, 4 female) versus GPER1-KO + G1: $95 \pm 4\%$ ($n = 12/6$ mice; 2 male, 4 female, $P = 0.001$, Mann-Whitney U test). (C) Quantitative analysis of input/output (I/O) curves, reflecting the stimulus-versus-response behavior (i.e., excitability) of Schaffer collateral synapses in CA1, revealed differences between genotypes (two-way ANOVA (genotype): $F(1,66) = 4.0$, $P = 0.05$), which were mainly due to a significantly reduced excitability in slices from WT compared to GPER1-KO males (C, fEPSP slope (mV/ms/V), KO male: 0.029 ± 0.003 ($n = 20/10$) versus WT males: 0.019 ± 0.002 ($n = 17/11$), $P = 0.002$). Among the female slices, significant differences only were apparent, if the cycle stage was considered (two-way ANOVA (cycle): $F(1,29) = 10.8$, $P = 0.003$). Thus, Schaffer collateral synapses in CA1 were significantly more excitable in slices, which derived from 'E2 high' GPER1-KO females, if compared to slices from all other females, among which slices from 'E2 low' GPER1-KOs showed the lowest excitability (C, fEPSP slope (mV/ms/V): KO E2 high: 0.034 ± 0.005 ($n = 6/4$) versus WT E2 high: 0.023 ± 0.002 ($n = 8/5$), $P = 0.007$; versus WT E2 low: 0.025 ± 0.001 ($n = 9/6$), $P = 0.02$; versus KO E2 low: 0.016 ± 0.002 ($n = 10/6$), $P < 0.001$). (D-H) Long-term potentiation (LTP) was induced by theta burst stimulation (TBS, 10 bursts of four 100 Hz pulses with 200 ms interburst intervals, arrows in D) and resulted in an initial increase of fEPSP slopes (level 1/L1 = 0–5 min post-TBS) in all experimental groups (D, E, G). No significant differences between genotypes, sexes, or cycle stages were detected at this level (E, G). After 30 minutes (level 2/L2 = 30–35 min post-TBS), potentiation had remained stable in slices from WT females (E; level 1: $174 \pm 7\%$, level 2: $183 \pm 13\%$ ($n = 19/14$), $P = 0.82$, Wilcoxon) and from GPER1-KO males (E; level 1: $169 \pm 8\%$, level 2: $153 \pm 8\%$ ($n = 11/8$), $P = 0.12$, Wilcoxon). However, in slices from WT males potentiation had significantly decayed (E; level 1: $172 \pm 7\%$, level 2: $152 \pm 6\%$ ($n = 12/9$), $P = 0.003$, Wilcoxon), whereas it had increased in the slices from GPER1-KO females (E; level 1: $175 \pm 5\%$, level 2: $193 \pm 7\%$ ($n = 14/8$), $P = 0.02$, paired t -test). Consequently, an effect of sex was noted (two-way ANOVA (sex): $F(1,52) = 8.1$, $P = 0.006$), if the differences between levels 1 and 2 (L2–L1) were compared, which was mainly due to increased potentiation at level 2 in slices from GPER1-KO females, if compared to those from WT and GPER1-KO males (F; L2–L1, KO female: $18 \pm 6\%$ ($n = 14/8$) versus WT male: $-20 \pm 5\%$ ($n = 12/9$), $P = 0.02$; versus KO male: $-16 \pm 12\%$, ($n = 11/8$), $P = 0.04$; but versus WT females: $9 \pm 13\%$, ($n = 19/14$), $P = 0.5$). Further, an effect of cycle was noted (two-way ANOVA (cycle): $F(1,29) = 9.2$, $P = 0.005$), which was due to increased potentiation at level 2 specifically in slices from 'E2 high' females (WT and GPER1-KO), in which L2–L1 differed significantly from values derived from 'E2 low' WT (H; L2–L1, WT E2 low: $-30 \pm 8\%$ ($n = 8/7$) versus WT E2 high: $37 \pm 18\%$ ($n = 11/7$), $P = 0.001$; versus KO E2 high: $27 \pm 7\%$, ($n = 7/4$), $P = 0.001$) but not from 'E2 low' GPER1-KO females (KO E2 low: $9 \pm 10\%$ ($n = 7/4$) versus WT E2 high: $37 \pm 18\%$ ($n = 11/7$), $P = 0.15$; versus KO E2 high: $27 \pm 7\%$, ($n = 7/4$), $P = 0.4$). Further of note: while potentiation at L2 was not significantly different from L1 for slices from WT 'E2 high' (G; level 1: $179 \pm 8\%$, level 2: $216 \pm 15\%$ ($n = 11/7$), $P = 0.07$, paired t -test) and GPER1-KO 'E2 low' females (G; level 1: $164 \pm 6\%$, level 2: $174 \pm 8\%$ ($n = 7/4$), $P = 0.4$, paired t -test), it was significantly increased in slices from KO 'E2 high' (G; level 1: $186 \pm 4\%$, level 2: $213 \pm 7\%$ ($n = 7/4$), $P = 0.007$, paired t -test) but decreased in slices from WT 'E2 low' females (G; level 1: $168 \pm 11\%$, level 2: $137 \pm 5\%$ ($n = 8/7$), $P = 0.009$, paired t -test). (I-K) Paired pulse ratio (PPR) was determined at interstimulus intervals 5, 10, 20, 50, 100, 200, and 500 ms. In these experiments, all experimental groups reduced PPR with increasing intervals (I). However, we noticed that the PPR in slices from GPER1-KO males tended to be lower compared to those from WT males. This difference proved to be significant, if interstimulus intervals were >100 ms (e.g., 200 ms, K; two-way ANOVA (interaction): $F(1,80) = 4.1$, $P = 0.045$; KO male: 1.14 ± 0.02 ($n = 14/5$) versus WT male: 1.26 ± 0.08 ($n = 11/4$), $P = 0.04$), but not if they were <100 ms (e.g., 50 ms, J). No significant differences were observed among slices from females, irrespective of cycle stage. Statistical details, which are not provided in the text, are available in the 'Supplementary Table 1.' Quantitative data in the text and in A, D, and I represent mean \pm S.E.M. Graphs in B, C, E–H, J, and K show box-and-whisker-plots (minimum–maximum) including all data points.

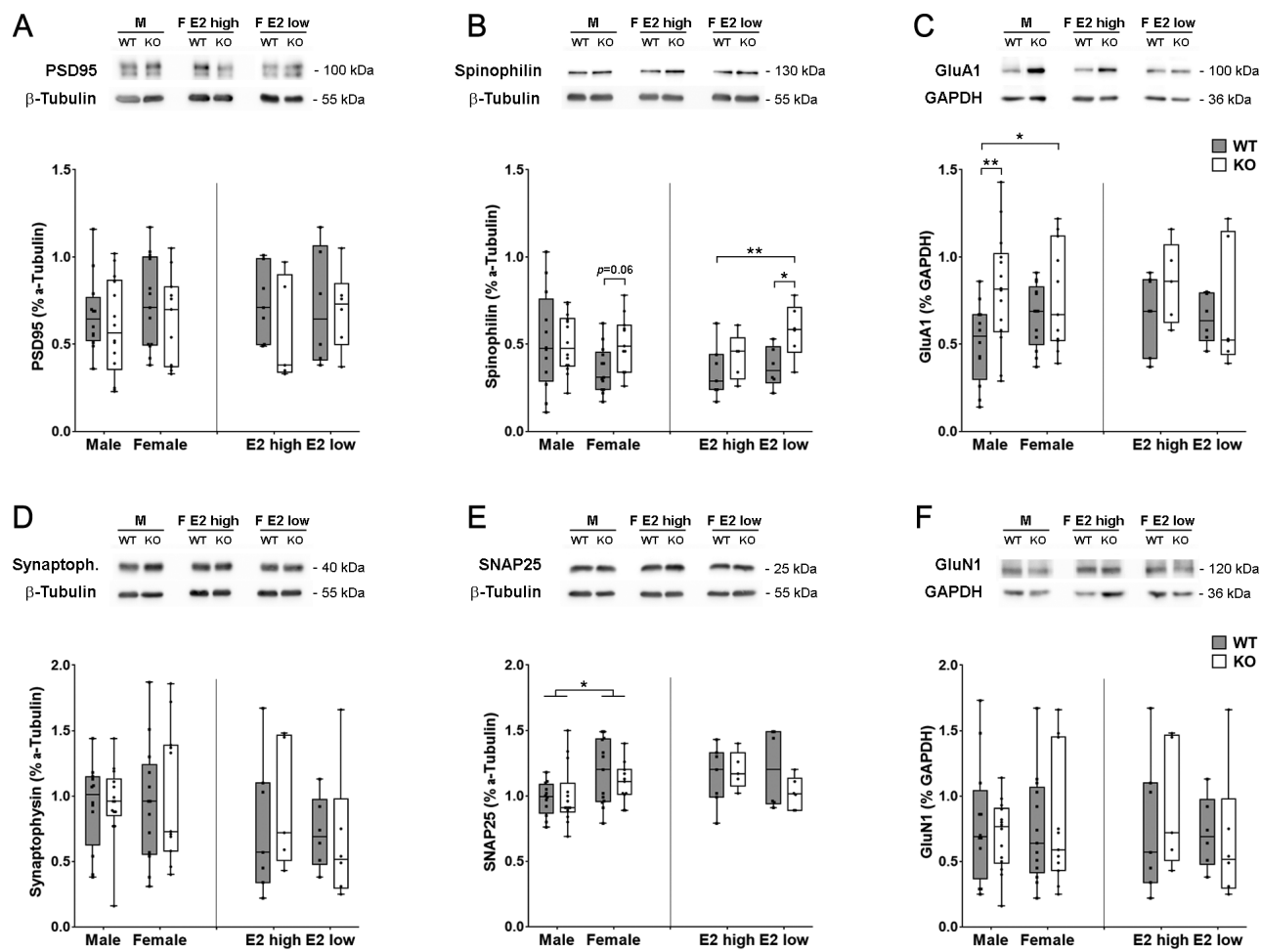
were derived from 'E2 low' females, the opposite effect was observed, resulting in a significant decrease of the I/O slope in GPER1-KO compared to WT female mice. Thus, the absence of the receptor had apparently caused a dysbalance in the GPER1-KOs, resulting in changes of CA1 excitability throughout the female cycle (Fig. 5C).

To pinpoint the underlying mechanism, we next examined postsynaptic properties by inducing LTP via TBS and found initially fEPSPs in CA1 equally increased in slices from GPER1-KO and WT mice (to 169–175% of baseline at level 1, without notable differences between experimental groups; Fig. 5D, E, and G). However, subsequent early maintenance of potentiation (E-LTP) strongly depended on genotype, sex, and cycle stage. Thus, while potentiation decreased within the following 30 min in slices from WT and GPER1-KO males, it remained stable in slices from WT females and increased significantly in slices from GPER1-KO females (level 2; Fig. 5E and F). Subsequent analysis of cycle effects (Fig. 5G and H) revealed that it is specifically the 'E2 high' stage, which strengthens E-LTP, as potentiation at level 2 was significantly increased in slices from both WT and GPER1-KO females, if compared to slices from 'E2 low' females (Fig. 5H). On the other side, while level

2 potentiation decreased below its initial value (level 1) in the slices from 'E2 low' WT females, it remained stable in 'E2 low' GPER1-KOs. These data confirm previous notions that E2 has a substantial impact on LTP (Warren *et al.* 1995, Bi *et al.* 2001), which appears not to be limited to LTP induction but may also include its maintenance. They further suggest that GPER1 has a regulatory function in this process, as the absence of the receptor resulted in an enhancement of E-LTP specifically in the females. We further performed paired-pulse experiments, asking whether the PPR is altered in slices from GPER1-KO mice, which could indicate presynaptic GPER1 functions (Fig. 5I). We noticed that PPR tended to be smaller in slices from GPER1-KO compared to WT males with significant differences at interstimulus intervals >100 ms (Fig. 5J and K). Significant differences in slices from females were not observed in these experiments, irrespective of the cycle stage.

Altered expression of synaptic proteins in hippocampus of GPER1-deficient mice

Altered synaptic properties usually involve an altered expression of synaptic proteins. Therefore, we next

**Figure 6**

Altered expression levels of hippocampal synaptic proteins in GPER1-KO mice. Quantitative Western Blot analyses were performed to determine hippocampal expression levels of synaptic proteins PSD95 (A), spinophilin (B), GluA1 (C), synaptophysin (D), SNAP25 (E) and NMDA-receptor subunit GluN1 (F). While no differences between genotypes were observed for PSD95, synaptophysin, SNAP25 and NMDA-receptor subunit GluN1, an effect of genotype was detected for the expression of AMPA-receptor subunit GluA1, which was significantly reduced in WT males compared to both GPER1-KO males and females (C; two-way ANOVA (genotype): $F(1,46)=7.3, P=0.01$; WT male: $0.51 \pm 0.07 (n=12)$ versus KO male: $0.81 \pm 0.09 (n=14), P=0.006$; versus KO female: $0.77 \pm 0.09 (n=11), P=0.02$; but versus WT female: $0.67 \pm 0.05 (n=13), P=0.15$; no difference was detected between cycle stages). An effect of genotype was further detected for spinophilin, if cycle stages were analyzed (B; two-way ANOVA (genotype): $F(1,20)=6.4, P=0.02$). Thus, spinophilin expression was significantly elevated in hippocampi from 'E2 low' GPER1-KO females, as compared to both 'E2 low' and 'E2 high' WT females (B; KO E2 low: $0.58 \pm 0.06 (n=6)$ versus WT E2 low: $0.37 \pm 0.05 (n=6), P=0.02$; versus WT E2 high: $0.34 \pm 0.06 (n=7), P=0.007$; but versus KO E2 high: $0.43 \pm 0.06 (n=5), P=0.09$). Generally, hippocampal spinophilin levels appeared enhanced in GPER1-KO compared to WT females, but this difference did not reach the level of significance (B; KO females: $0.51 \pm 0.05 (n=11)$ versus WT females: $0.36 \pm 0.04 (n=13), P=0.06$). No difference was detected among the males (B; KO males: $0.5 \pm 0.04 (n=14)$ versus WT males: $0.52 \pm 0.08 (n=12), P=0.86$). Additionally, an effect of sex was detected for the expression of SNAP25 (E; two-way ANOVA (sex): $F(1,46)=7.0, P=0.01$), as hippocampal SNAP25 levels were significantly enhanced in WT females compared to both WT and GPER1-KO males (WT female: $1.18 \pm 0.07 (n=13)$ versus WT male: $0.98 \pm 0.04 (n=12), P=0.02$; versus KO male: $1.00 \pm 0.06 (n=14), P=0.02$ but versus KO female: $1.1 \pm 0.05 (n=11), P=0.35$). However, no difference between genotypes was observed here. Insets show representative blots for the synaptic proteins analyzed. Note in (A): two bands running tightly below resp. above 100 kDa were regularly observed with the chosen PSD95 antibody, indicative of post-translationally modified PSD95 isoforms (Yokoi *et al.* 2016, Vallejo *et al.* 2017). Both bands were combined for analysis. Quantitative data in the text represent mean \pm S.E.M. Graphs show box-and-whisker-plots (minimum–maximum) including all data points. Statistical details, which are not provided in the text, are available in the 'Supplementary Table 1.'

examined the expression levels of synaptic proteins, which have previously been shown to be regulated by estrogens, in the hippocampus of naive animals (which were not used for behavior testing). Specifically, expression levels of postsynaptic PSD95 (Akama *et al.*

2013, Li *et al.* 2021) and spinophilin (Li *et al.* 2004, Fester *et al.* 2009), presynaptic SNAP25 (Pechenino & Frick 2009) and synaptophysin (Fester *et al.* 2009), and glutamate receptor subunits GluA1 (Srivastava *et al.* 2008) and GluN1 (Brandt *et al.* 2020) were analyzed and compared

between GPER1-KO and WT mice. In these analyses, we did not detect differences between genotypes for PSD95 (Fig. 6A), synaptophysin (Fig. 6D), SNAP25 (Fig. 6E) and NMDA receptor subunit GluN1 (Fig. 6F). However, an effect of genotype was indicated for the expression of AMPA-receptor subunit GluA1, which was significantly increased in GPER1-KO males and females compared to WT males (Fig. 6C). An effect of genotype was further detected for spinophilin, as hippocampal spinophilin expression was increased in GPER1-KO compared to WT females, specifically if they were in an 'E2 low' cycle stage (Fig. 6B). Further of note: an effect of sex was detected for the expression of SNAP25 (Fig. 6E).

Discussion

Since its discovery (Carmeci *et al.* 1997), a multitude of studies have investigated the functions of GPER1, which is abundantly expressed in the brain, including the hippocampus (Matsuda *et al.* 2008, Akama *et al.* 2013, Waters *et al.* 2015, Meseke *et al.* 2018, Wang *et al.* 2018, Llorente *et al.* 2020). Most of these studies involved the exogenous application of receptor agonists or antagonists, thus providing ample evidence that this treatment influences cognitive functions (Alexander *et al.* 2017, Hadjimarkou & Vasudevan 2018, Taxier *et al.* 2020). For hippocampus-related functions, such as spatial or object-related memory, activation of GPER1 has been found to be favorable (Kim *et al.* 2016, Lymer *et al.* 2017), whereas inhibition of GPER1 resulted in impairment of memory (Hammond *et al.* 2012, Kim *et al.* 2016). Using GPER1-deficient mice (Wang *et al.* 2008) to study the roles of the receptor in the hippocampus, we here provide support for the assumption that GPER1 is involved in the acquisition of memory, but the underlying mechanisms may be more complex than thought and may be sex-specifically regulated. Our major findings are (1) while GPER1-KO mice overall performed poorer compared to WT mice in the MWM, deficits were among the females more pronounced in stages of the estrous cycle, during which E2 serum levels are rising or high ('E2 high') compared to those, in which E2 levels were low or declining ('E2 low'; (Frick *et al.* 2015, Nilsson *et al.* 2015). (2) Similarly, in CFC, GPER1-KO females showed a stronger freezing response compared to WT females and males of both genotypes, specifically if they were in a 'E2 high' stage of the estrous cycle. (3) On the physiological level, we noted enhanced excitability of Schaffer collateral

synapses in GPER1-KO males and 'E2 high' females, which correlates with an increased hippocampal expression of AMPA receptor subunit GluA1 in GPER1-KO males and females, if compared to WT males. In addition, E-LTP, which is generally enhanced, if E2 serum levels are high, appears to be more stable, if GPER1 is absent. Further findings include a lesser anxiety of GPER1-KO males in EPM, a reduced PPR at interstimulus intervals >100 ms specifically in slices from GPER1-KO males, and an increased hippocampal expression of spinophilin in GPER1-KO females (specifically if E2 levels were low). Taken together, these findings strengthen the notion that GPER1 mediates E2-related effects – at least in females. However, they further suggest that within the hippocampal network GPER1 decreases, rather than increases, excitability and may thus have a modulatory role, for which sex-specific regulatory mechanisms may apply. Further of note: our behavior data generally agree with the results of a recent study using GPER1-KO rats (Zheng *et al.* 2020). These authors also examined spatial learning in an MWM and found an increased latency to reach the target and a decreased time at the target for both GPER1-KO males and females. However, the authors used ovariectomized females and did not distinguish between cycle stages in this part of their study.

There is an extensive body of evidence that estrogens – particularly its most potent form E2 – influence functional synaptic plasticity in the rodent hippocampus. On the morphological level, the circulating estrogen state is positively correlated with the total number of spines in hippocampal CA1 (Woolley *et al.* 1990, Sheppard *et al.* 2019) and with the proportion of mushroom-shaped spines, which are considered the 'memory spines' (Li *et al.* 2004, Brandt *et al.* 2020). Further, on the physiological level, high E2-levels are positively correlated with the magnitude of field CA1 LTP (Warren *et al.* 1995, Bi *et al.* 2001), involving an increase in NMDA receptor-mediated transmission (Smith & McMahon 2005). In addition, E2 conveys rapid effects on synaptic excitability, occurring within minutes, which do not require protein synthesis and involve the rapid insertion of extrasynaptic AMPA receptors into synaptic sites (Srivastava *et al.* 2008, Kramár *et al.* 2009). In this respect, it is noteworthy that we found higher expression levels of the constitutive AMPA-receptor subunit GluA1 (but not of NMDA-receptor subunit GluN1) both in GPER1-KO male and female compared to WT male mice, suggesting that increased availability of AMPA receptors could underlie the increased excitability in CA1 that was observed in slices from GPER1-KO males and in those

from GPER1-KO females if they had been in an 'E2 high' stage (Fig. 5C). This implicates that GPER1, if present and activated, constraints AMPA receptor expression – a hypothesis that is supported by the finding that G1 infusion attenuates stress-induced GluA1 expression in the basolateral amygdala (Tian *et al.* 2013). However, an alternative explanation for the increased excitability of the Schaffer collateral synapses could be provided by presynaptic changes, which lead to an enhanced transmitter release upon stimulation. Indeed, a lower paired-pulse ratio was found for GPER1-KO compared to WT males at interstimulus intervals >100, which would generally be concordant with such a scenario. However, expression analyses of vesicle-associated presynaptic proteins did not support this option, as hippocampal expression levels of SNAP25 and synaptophysin did not correlate with the observed PPR differences. Further, alterations in PPR can also result from postsynaptic changes, such as an altered availability of synaptic glutamate receptors (Bagal *et al.* 2005, Moult *et al.* 2006), as it appears to be the case for the GPER1-KO males. Nevertheless, presynaptic changes should not generally be excluded, as hippocampal SNAP25 expression has been shown to be responsive to E2 in adult female mice (Pechenino & Frick 2009).

In addition to increased excitability, E-LTP was found to be more stable in slices from GPER1-KO compared to WT mice – a phenomenon not explained by increased availability of AMPA-receptors alone, as it was explicitly seen in females (Fig. 5D, E, F, G, and H). E-LTP denotes the first 1–6 h after LTP initiation, during which LTP decays if it is not stabilized (Becker & Tetzlaff 2021). Maintenance of E-LTP is considered to be mostly protein synthesis independent. Still, it involves the membrane insertion of intracellular AMPA receptors via exocytosis and their trapping in the postsynaptic density, combined with alterations of spine morphology, which require integrin-mediated interactions with the extracellular matrix and intracellular actin polymerization (Babayan *et al.* 2012, Becker & Tetzlaff 2021). Our data do not yet provide insight into the mechanisms of E-LTP stabilization that could involve GPER1. However, our observation that the expression of spinophilin is increased in GPER1-KO relative to WT females (Fig. 6B) could provide a hint, as spinophilin is a spine-associated protein that interacts with actin and modulates the functions of postsynaptic receptors via protein phosphatase 1 (Foley *et al.* 2021). Further, the expression of spinophilin is influenced by E2 (Li *et al.* 2004,

Fester *et al.* 2009) and may thus participate in the E2-mediated regulation of LTP. The specific roles of spinophilin for E2-mediated plasticity await further elucidation, but it is known to regulate the activity of G-protein-coupled receptors, such as muscarinic acetylcholine receptors (Kurogi *et al.* 2009, Ruiz de Azua *et al.* 2012), which modulate hippocampal network activity via mechanisms that involve GPER1 functions (Fuenzalida *et al.* 2021). In contrast, hippocampal expression of PSD95, which was previously shown to interact with GPER1 (Akama *et al.* 2013), was not found to be altered in the GPER1-KOs. Further of note: our finding of an altered E-LTP maintenance in GPER1-KO female slices is discrepant with the observation that application of the GPER1 antagonist G15 does not alter Schaffer collateral LTP maintenance in slices from adolescent female rats (Wang *et al.* 2018). However, the younger age of the animals used in this study and species effects could account for this discrepancy.

Besides deficits in the MWM, we noticed sex-specific effects related to anxiety and fear in GPER1-KO mice. Thus, GPER1-KO males, but not females, spent more time in open arms compared to WT males and females in the EPM, indicating lesser anxiety specifically of the GPER1-KO males, whereas 'E2 high' GPER1-KO females showed an increased fear response in the CFC paradigm. These observations are largely in agreement with findings in other GPER1-KO models. Thus, analogous to our data, reduced anxiety in the EPM by male, but not female, GPER1-KO mice was observed in a different GPER1-deficient mouse line (Kastenberger & Schwarzer 2014). Similarly, in the study by Zheng and colleagues, female GPER1-KO rats showed significantly less exploratory behavior compared to GPER1-KO males in the EPM, although these did not perform better than the WT rats (Zheng *et al.* 2020). Our observations are also consistent with reports showing anxiogenic effects of a single subcutaneous injection of G1 in ovariectomized female and intact male mice (Kastenberger *et al.* 2012) but are discrepant with reports stating anxiolytic effects of a single dose of G1 in castrated male (Hart *et al.* 2014) and of chronically applied G1 in ovariectomized female mice (Anchan *et al.* 2014). Overall, these findings suggest functions of GPER1 in networks which govern anxiety, including the hippocampus and the amygdala, in which GPER1 is substantially expressed (Tian *et al.* 2013, Llorente *et al.* 2020, Zheng *et al.* 2020). Remarkably, in these networks, GPER1 signaling appears to constrain competing effects of E2, mediated presumably via

ER α and β (Lund *et al.* 2005, Tetel & Pfaff 2010), because differences between genotypes specifically become evident if E2 levels are high. Indeed, anxiety behavior appears to depend on estrogen levels, as high E2 concentrations were reported to be anxiolytic, whereas low levels often cause anxiogenic effects in female rodents (Toufexis *et al.* 2006). GPER1 could thus act anxiolytic if E2 levels are high, but anxiogenic if levels are low (such as it is naturally the case in males). Competing actions of other receptor types (which may also include androgen receptors) could further explain some of the above-named discrepancies, as influences of peripheral sex hormones had largely been removed in these studies (by ovariectomizing females resp. castrating males), and levels of sexual hormones were thus naturally low. Alternatively, altered levels of stress hormones due to dysregulation of the hypothalamic–pituitary–adrenal (HPA) axis specifically in GPER1-KO females were suggested as an explanation for the emerging sex differences (Zheng *et al.* 2020). However, while these may play a role, we do not think that they can fully account for the sex-specific differences that we observed in our study because we did not observe differences between genotypes or sexes, if stress indicators like grooming, rearing, or the number of feces dropped were analyzed.

In summary, we undertook a comprehensive study of GPER1 functions in hippocampus-related processes using a GPER1-deficient mouse line. While our data partially replicate what is already known from other studies, their novelty lies in the fact that we have used both sexes and considered the female estrous cycle, thus being able to point out sex differences and to highlight the impact of E2 influence. Most importantly, our data indicate that GPER1 does not merely increase synaptic activity in CA1 upon activation, as suggested by experiments (including ours) using G1 in hippocampal slices (Fig. 5A and B; Lebesgue *et al.* 2009, Kumar *et al.* 2015). They, in contrast, suggest a modulatory role of GPER1 in the CA1 network, as CA1 excitability was reduced and E-LTP-maintenance was weakened in WT compared to GPER1-KO slices. While these findings – increased excitability with G1, but otherwise reduced excitability in the WT slices – seem to be in conflict with each other, one should keep in mind that exogenous agonists are usually not applied in concentrations of the endogenous ligands and may thus induce effects that demonstrate the functionality of the receptor (as intended here) but do not necessarily reflect its physiological functions truly. Comparing GPER1-KO mice to WT litter mates

thus appears to be more appropriate to pinpoint GPER1 functions, although this approach carries the risk of compensatory mechanisms, which may disguise the true effects of GPER1-deficiency. Optimally, inducible GPER1-KO mice should have been used, which were, however, not available for this study. Keeping these confounders in mind, our hypothesis receives support by the observation that G1 promotes LTD in CA3 via mTOR-mediated internalization of GluA1 subunits (Briz *et al.* 2015, Xu *et al.* 2018). No effect of G1 on CA1 LTD has been observed in these studies, but the roles of E2 in CA1 LTD are not yet finally resolved (Murakami *et al.* 2015, Tozzi *et al.* 2019) and may merit a closer look at the contribution of GPER1.

Further, how effects of GPER1-deficiency on CA1 plasticity and synaptic protein expression translate into the observed behavioral changes remains to be resolved. On the physiological level, memory encoding (i.e., learning) has been tightly linked to LTP, which in CA1 involves activation of Ca^{2+} -permeable NMDA-receptors, followed by incorporation of extrasynaptic AMPA receptors into postsynaptic sites (Martin & Clark 2007, Srivastava *et al.* 2008, Gall *et al.* 2021). An increased availability of GluA1 subunits in GPER1-KO mice could thus promote CA1 LTP and consequently learning. This is not what we observed, as GPER1-KO performed poorer than WT mice in the MWM learning, long-term and remote probe trials, suggesting that consolidation and/or retrieval of spatial memory is affected. Proper memory encoding is, however, a multifactorial process that not only requires the hippocampal network but also depends on its interaction with extra-hippocampal sites such as the septal region, the amygdala, or the cortex (Martin & Clark 2007, Gall *et al.* 2021), which are themselves subject to GPER1-mediated regulation (Tian *et al.* 2013, Gibbs *et al.* 2014, Bender *et al.* 2017). As these regions have not yet been analyzed in detail, we can presently only speculate that the absence of GPER1 causes a dysregulation of these intricate interactions, resulting in the genotype-specific deficits observed in the MWM and in the differences with respect to fear- and anxiety-related behavior.

Similarly, in view of ample evidence that E2 promotes LTP and spine formation in hippocampus (Woolley *et al.* 1990, Warren *et al.* 1995, Bi *et al.* 2001, Kramár *et al.* 2009, Sheppard *et al.* 2019), it is remarkable that 'E2 high' WT females did not perform better in the MWM compared to 'E2 low' WT females, whereas differences between cycle stages became evident among the GPER1-KOs. However, these observations are not

that unexpected if one considers that previous studies did not find clear-cut positive correlations between E2 serum levels and hippocampus-dependent spatial memory acquisition in WT rodents but observed either modestly improved performances during proestrus (Frick & Berger-Sweeney 2001), negative effects of high E2 on spatial reference memory (Warren & Juraska 1997, Pompili *et al.* 2010) or no effect at all (Berry *et al.* 1997, Stackman *et al.* 1997). This apparent paradox may be explained by the fact that serum E2 is not the major source of hippocampal E2, which mainly derives from neuronal aromatase that is abundantly expressed in the hippocampus (Hojo *et al.* 2008, Fester & Rune 2015). Hippocampal aromatase activity is subject to negative feed-back regulation via the hypothalamus–pituitary–gonadal axis (Prange-Kiel *et al.* 2008) and is further regulated by neuronal activity (Fester *et al.* 2016), thus eventually mediating a homeostatic adaptation of hippocampal E2 levels to the demands of the hippocampal network. We propose a related role for GPER1: by attenuating E2-mediated excitability, it could support homeostatic adaptation within the hippocampal network, which gets dysregulated, if GPER1 is absent.

Supplementary materials

This is linked to the online version of the paper at <https://doi.org/10.1530/JOE-22-0204>.

Declaration of interest

The authors declare that there is no conflict of interest that could be perceived as prejudicing the impartiality of the research reported.

Funding

This study was financially supported by the Deutsche Forschungsgemeinschaft (DFG; RAB: Be4107/3-1; GMR: Ru436/7-1). XL was supported by a scholarship from China Scholarship Council.

Author contribution statement

AK – performed electrophysiology, YK – performed behavior studies and Western blots, XL – established GPER1-KO line and performed Western Blots, FM – planned and supervised behavior studies, GMR – designed experiments, RAB – designed experiments and wrote the paper.

Acknowledgements

We wish to thank Drs Christine Gee, Ora Ohana and Bianka Brunne for methodological advice, and J Graw, H Hamann, H Herbort, K Sander and C Schröder-Birkner for excellent technical assistance.

References

- Akama KT, Thompson LI, Milner TA & McEwen BS 2013 Post-synaptic density-95 (PSD-95) binding capacity of G-protein-coupled receptor 30 (GPR30), an estrogen receptor that can be identified in hippocampal dendritic spines. *Journal of Biological Chemistry* **288** 6438–6450. (<https://doi.org/10.1074/jbc.M112.412478>)
- Albo Z & Gräff J 2018 The mysteries of remote memory. *Philosophical Transactions of the Royal Society of London. Series B, Biological Sciences* **373** 20170029. (<https://doi.org/10.1098/rstb.2017.0029>)
- Alexander A, Irving AJ & Harvey J 2017 Emerging roles for the novel estrogen-sensing receptor GPER1 in the CNS. *Neuropharmacology* **113** 652–660. (<https://doi.org/10.1016/j.neuropharm.2016.07.003>)
- Anchan D, Clark S, Pollard K & Vasudevan N 2014 GPR30 activation decreases anxiety in the open field test but not in the elevated plus maze test in female mice. *Brain and Behavior* **4** 51–59. (<https://doi.org/10.1002/brb3.197>)
- Babayan AH, Kramár EA, Barrett RM, Jafari M, Häettig J, Chen LY, Rex CS, Lauterborn JC, Wood MA, Gall CM, *et al.* 2012 Integrin dynamics produce a delayed stage of long-term potentiation and memory consolidation. *Journal of Neuroscience* **32** 12854–12861. (<https://doi.org/10.1523/JNEUROSCI.2024-12.2012>)
- Bagal AA, Kao JP, Tang CM & Thompson SM 2005 Long-term potentiation of exogenous glutamate responses at single dendritic spines. *Proceedings of the National Academy of Sciences of the United States of America* **102** 14434–14439. (<https://doi.org/10.1073/pnas.0501956102>)
- Becker MFP & Tetzlaff C 2021 The biophysical basis underlying the maintenance of early phase long-term potentiation. *PLOS Computational Biology* **17** e1008813. (<https://doi.org/10.1371/journal.pcbi.1008813>)
- Bender RA, Zhou L, Vierk R, Brandt N, Keller A, Gee CE, Schafer MK & Rune GM 2017 Sex-dependent regulation of aromatase-mediated synaptic plasticity in the basolateral amygdala. *Journal of Neuroscience* **37** 1532–1545. (<https://doi.org/10.1523/JNEUROSCI.1532-16.2016>)
- Berry B, McMahan R & Gallagher M 1997 Spatial learning and memory at defined points of the estrous cycle: effects on performance of a hippocampal-dependent task. *Behavioral Neuroscience* **111** 267–274. (<https://doi.org/10.1037/0735-7044.111.2.267>)
- Bi R, Foy MR, Vouimba RM, Thompson RF & Baudry M 2001 Cyclic changes in estradiol regulate synaptic plasticity through the MAP kinase pathway. *Proceedings of the National Academy of Sciences of the United States of America* **98** 13391–13395. (<https://doi.org/10.1073/pnas.241507698>)
- Bolles RC 1970 Species-specific defense reactions and avoidance learning. *Psychological Review* **77** 32–48. (<https://doi.org/10.1037/h0028589>)
- Bologa CG, Revankar CM, Young SM, Edwards BS, Arterburn JB, Kiselyov AS, Parker MA, Tkachenko SE, Savchuck NP, Sklar LA, *et al.* 2006 Virtual and biomolecular screening converge on a selective agonist for GPR30. *Nature Chemical Biology* **2** 207–212. (<https://doi.org/10.1038/nchembio775>)
- Brailoiu E, Dun SL, Brailoiu GC, Mizuo K, Sklar LA, Oprea TI, Prossnitz ER & Dun NJ 2007 Distribution and characterization of estrogen receptor G protein-coupled receptor 30 in the rat central nervous system. *Journal of Endocrinology* **193** 311–321. (<https://doi.org/10.1677/JOE-07-0017>)
- Brandt N, Löffler T, Fester L & Rune GM 2020 Sex-specific features of spine densities in the hippocampus. *Scientific Reports* **10** 11405. (<https://doi.org/10.1038/s41598-020-68371-x>)
- Briz V, Liu Y, Zhu G, Bi X & Baudry M 2015 A novel form of synaptic plasticity in field CA3 of hippocampus requires GPER1 activation and BDNF release. *Journal of Cell Biology* **210** 1225–1237. (<https://doi.org/10.1083/jcb.201504092>)
- Carmeci C, Thompson DA, Ring HZ, Francke U & Weigel RJ 1997 Identification of a gene (GPR30) with homology to the G-protein-coupled receptor superfamily associated with estrogen receptor expression in breast cancer. *Genomics* **45** 607–617. (<https://doi.org/10.1006/geno.1997.4972>)
- Dennis MK, Burai R, Ramesh C, Petrie WK, Alcon SN, Nayak TK, Bologa CG, Leitao A, Brailoiu E, Deliu E, *et al.* 2009 In vivo effects of a GPR30 antagonist. *Nature Chemical Biology* **5** 421–427. (<https://doi.org/10.1038/nchembio.168>)

- Dennis MK, Field AS, Burai R, Ramesh C, Petrie WK, Bologa CG, Oprea TI, Yamaguchi Y, Hayashi S, Sklar LA, *et al.* 2011 Identification of a GPER/GPR30 antagonist with improved estrogen receptor counterselectivity. *Journal of Steroid Biochemistry and Molecular Biology* **127** 358–366. (<https://doi.org/10.1016/j.jsbmb.2011.07.002>)
- Fellini L, Schachner M & Morellini F 2006 Adult but not aged C57BL/6 male mice are capable of using geometry for orientation. *Learning and Memory* **13** 473–481. (<https://doi.org/10.1101/lm.259206>)
- Fester L, Zhou L, Butow A, Huber C, von Lossow R, Prange-Kiel J, Jarry H & Rune GM 2009 Cholesterol-promoted synaptogenesis requires the conversion of cholesterol to estradiol in the hippocampus. *Hippocampus* **19** 692–705. (<https://doi.org/10.1002/hipo.20548>)
- Fester L & Rune GM 2015 Sexual neurosteroids and synaptic plasticity in the hippocampus. *Brain Research* **1621** 162–169. (<https://doi.org/10.1016/j.brainres.2014.10.033>)
- Fester L, Brandt N, Windhorst S, Prols F, Blaute C & Rune GM 2016 Control of aromatase in hippocampal neurons. *Journal of Steroid Biochemistry and Molecular Biology* **160** 9–14. (<https://doi.org/10.1016/j.jsbmb.2015.10.009>)
- Foley K, McKee C, Nairn AC & Xia H 2021 Regulation of synaptic transmission and plasticity by protein phosphatase 1. *Journal of Neuroscience* **41** 3040–3050. (<https://doi.org/10.1523/JNEUROSCI.2026-20.2021>)
- Frick KM & Berger-Sweeney J 2001 Spatial reference memory and neocortical neurochemistry vary with the estrous cycle in C57BL/6 mice. *Behavioral Neuroscience* **115** 229–237. (<https://doi.org/10.1037/0735-7044.115.1.229>)
- Frick KM, Kim J, Tuscher JJ & Fortress AM 2015 Sex steroid hormones matter for learning and memory: estrogenic regulation of hippocampal function in male and female rodents. *Learning and Memory* **22** 472–493. (<https://doi.org/10.1101/lm.037267.114>)
- Fuenzalida M, Chiu CQ & Chávez AE 2021 Muscarinic regulation of spike timing dependent synaptic plasticity in the hippocampus. *Neuroscience* **456** 50–59. (<https://doi.org/10.1016/j.neuroscience.2020.08.015>)
- Funakoshi T, Yanai A, Shinoda K, Kawano MM & Mizukami Y 2006 G Protein-coupled receptor 30 is an estrogen receptor in the plasma membrane. *Biochemical and Biophysical Research Communications* **346** 904–910. (<https://doi.org/10.1016/j.bbrc.2006.05.191>)
- Gabor C, Lymer J, Phan A & Choleris E 2015 Rapid effects of the G-protein coupled oestrogen receptor (GPER) on learning and dorsal hippocampus dendritic spines in female mice. *Physiology and Behavior* **149** 53–60. (<https://doi.org/10.1016/j.physbeh.2015.05.017>)
- Gall CM, Le AA & Lynch G 2021 Sex differences in synaptic plasticity underlying learning. *Journal of Neuroscience Research* **101** 764–782. (<https://doi.org/10.1002/jnr.24844>)
- Gibbs RB, Nelson D & Hammond R 2014 Role of GPR30 in mediating estradiol effects on acetylcholine release in the hippocampus. *Hormones and Behavior* **66** 339–345. (<https://doi.org/10.1016/j.yhbeh.2014.06.002>)
- Haas E, Bhattacharya I, Brailoiu E, Damjanović M, Brailoiu GC, Gao X, Mueller-Guerre L, Marjon NA, Gut A, Minotti R, *et al.* 2009 Regulatory role of G protein-coupled estrogen receptor for vascular function and obesity. *Circulation Research* **104** 288–291. (<https://doi.org/10.1161/CIRCRESAHA.108.190892>)
- Hadjimarkou MM & Vasudevan N 2018 GPER1/GPR30 in the brain: crosstalk with classical estrogen receptors and implications for behavior. *Journal of Steroid Biochemistry and Molecular Biology* **176** 57–64. (<https://doi.org/10.1016/j.jsbmb.2017.04.012>)
- Hammond R, Nelson D, Kline E & Gibbs RB 2012 Chronic treatment with a GPR30 antagonist impairs acquisition of a spatial learning task in young female rats. *Hormones and Behavior* **62** 367–374. (<https://doi.org/10.1016/j.yhbeh.2012.07.004>)
- Hart D, Nilges M, Pollard K, Lynn T, Patsos O, Shiel C, Clark SM & Vasudevan N 2014 Activation of the G-protein coupled receptor 30 (GPR30) has different effects on anxiety in male and female mice. *Steroids* **81** 49–56. (<https://doi.org/10.1016/j.steroids.2013.11.004>)
- Hawley WR, Grissom EM, Moody NM, Dohanich GP & Vasudevan N 2014 Activation of G-protein-coupled receptor 30 is sufficient to enhance spatial recognition memory in ovariectomized rats. *Behavioural Brain Research* **262** 68–73. (<https://doi.org/10.1016/j.bbr.2014.01.006>)
- Hazell GG, Yao ST, Roper JA, Prossnitz ER, O'Carroll AM & Lolait SJ 2009 Localisation of GPR30, a novel G protein-coupled oestrogen receptor, suggests multiple functions in rodent brain and peripheral tissues. *Journal of Endocrinology* **202** 223–236. (<https://doi.org/10.1677/JOE-09-0066>)
- Hojo Y, Murakami G, Mukai H, Higo S, Hatanaka Y, Ogiue-Ikeda M, Ishii H, Kimoto T & Kawato S 2008 Estrogen synthesis in the brain—role in synaptic plasticity and memory. *Molecular and Cellular Endocrinology* **290** 31–43. (<https://doi.org/10.1016/j.mce.2008.04.017>)
- Izquierdo I, Furini CR & Myskiw JC 2016 Fear memory. *Physiological Reviews* **96** 695–750. (<https://doi.org/10.1152/physrev.00018.2015>)
- Kastenberger I, Lutsch C & Schwarzer C 2012 Activation of the G-protein-coupled receptor GPR30 induces anxiogenic effects in mice, similar to oestradiol. *Psychopharmacology* **221** 527–535. (<https://doi.org/10.1007/s00213-011-2599-3>)
- Kastenberger I & Schwarzer C 2014 GPER1 (GPR30) knockout mice display reduced anxiety and altered stress response in a sex and paradigm-dependent manner. *Hormones and Behavior* **66** 628–636. (<https://doi.org/10.1016/j.yhbeh.2014.09.001>)
- Kim J, Schalk JC, Koss WA, Gremminger RL, Taxier LR, Gross KS & Frick KM 2019 Dorsal hippocampal actin polymerization is necessary for activation of G-protein-coupled estrogen receptor (GPER) to increase CA1 dendritic spine density and enhance memory consolidation. *Journal of Neuroscience* **39** 9598–9610. (<https://doi.org/10.1523/JNEUROSCI.2687-18.2019>)
- Kim J, Szinte JS, Boulware MI & Frick KM 2016 17 β -estradiol and agonism of G-protein-coupled estrogen receptor enhance hippocampal memory via different cell-signaling mechanisms. *Journal of Neuroscience* **36** 3309–3321. (<https://doi.org/10.1523/JNEUROSCI.0257-15.2016>)
- Kramár EA, Chen LY, Brandon NJ, Rex CS, Liu F, Gall CM & Lynch G 2009 Cytoskeletal changes underlie estrogen's acute effects on synaptic transmission and plasticity. *Journal of Neuroscience* **29** 12982–12993. (<https://doi.org/10.1523/JNEUROSCI.3059-09.2009>)
- Kumar A, Bean LA, Rani A, Jackson T & Foster TC 2015 Contribution of estrogen receptor subtypes, ER α , ER β , and GPER1 in rapid estradiol-mediated enhancement of hippocampal synaptic transmission in mice. *Hippocampus* **25** 1556–1566. (<https://doi.org/10.1002/hipo.22475>)
- Kurogi M, Nagatomo K, Kubo Y & Saitoh O 2009 Effects of spinophilin on the function of RGS8 regulating signals from M2 and M3-mAChRs. *NeuroReport* **20** 1134–1139. (<https://doi.org/10.1097/WNR.0b013e32832fd93e>)
- Lebesgue D, Chevaleyre V, Zukin RS & Etgen AM 2009 Estradiol rescues neurons from global ischemia-induced cell death: multiple cellular pathways of neuroprotection. *Steroids* **74** 555–561. (<https://doi.org/10.1016/j.steroids.2009.01.003>)
- Li C, Brake WG, Romeo RD, Dunlop JC, Gordon M, Buzescu R, Magarinos AM, Allen PB, Greengard P, Luine V, *et al.* 2004 Estrogen alters hippocampal dendritic spine shape and enhances synaptic protein immunoreactivity and spatial memory in female mice. *Proceedings of the National Academy of Sciences of the United States of America* **101** 2185–2190. (<https://doi.org/10.1073/pnas.0307313101>)
- Li X, Johann S, Rune GM & Bender RA 2021 Sex-specific regulation of spine density and synaptic proteins by G-protein-coupled estrogen receptor (GPER)1 in developing hippocampus. *Neuroscience* **472** 35–50. (<https://doi.org/10.1016/j.neuroscience.2021.07.035>)
- Llorente R, Marraudino M, Carrillo B, Bonaldo B, Simon-Areces J, Abellanas-Pérez P, Rivero-Aguilar M, Fernandez-Garcia JM, Pinos H, Garcia-Segura LM, *et al.* 2020 G-protein-coupled estrogen receptor immunoreactivity fluctuates during the estrous cycle and shows sex differences in the amygdala and dorsal hippocampus. *Frontiers in Endocrinology (Lausanne)* **11** 537. (<https://doi.org/10.3389/fendo.2020.00537>)

- Lund TD, Rovis T, Chung WC & Handa RJ 2005 Novel actions of estrogen receptor-beta on anxiety-related behaviors. *Endocrinology* **146** 797–807. (<https://doi.org/10.1210/en.2004-1158>)
- Lymer J, Robinson A, Winters BD & Choleris E 2017 Rapid effects of dorsal hippocampal G-protein coupled estrogen receptor on learning in female mice. *Psychoneuroendocrinology* **77** 131–140. (<https://doi.org/10.1016/j.psyneuen.2016.11.019>)
- Martin SJ & Clark RE 2007 The rodent hippocampus and spatial memory: from synapses to systems. *Cellular and Molecular Life Sciences* **64** 401–431. (<https://doi.org/10.1007/s00018-007-6336-3>)
- Matsuda K, Sakamoto H, Mori H, Hosokawa K, Kawamura A, Itose M, Nishi M, Prossnitz ER & Kawata M 2008 Expression and intracellular distribution of the G-protein-coupled receptor 30 in rat hippocampal formation. *Neuroscience Letters* **441** 94–99. (<https://doi.org/10.1016/j.neulet.2008.05.108>)
- McLean AC, Valenzuela N, Fai S & Bennett SA 2012 Performing vaginal lavage, crystal violet staining, and vaginal cytological evaluation for mouse estrous cycle staging identification. *Journal of Visualized Experiments* **67** e4389. (<https://doi.org/10.3791/4389>)
- Meseke M, Neumüller F, Brunne B, Li X, Anstötz M, Pohlkamp T, Rogalla MM, Herz J, Rune GM & Bender RA 2018 Distal dendritic enrichment of HCN1 channels in hippocampal CA1 is promoted by estrogen, but does not require reelin. *eNeuro* **5**. (<https://doi.org/10.1523/JNEUROSCI.0258-18.2018>)
- Moult PR, Gladding CM, Sanderson TM, Fitzjohn SM, Bashir ZI, Molnar E & Collingridge GL 2006 Tyrosine phosphatases regulate AMPA receptor trafficking during metabotropic glutamate receptor-mediated long-term depression. *Journal of Neuroscience* **26** 2544–2554. (<https://doi.org/10.1523/JNEUROSCI.4322-05.2006>)
- Murakami G, Hojo Y, Ogiue-Ikeda M, Mukai H, Chambon P, Nakajima K, Ooishi Y, Kimoto T & Kawato S 2015 Estrogen receptor KO mice study on rapid modulation of spines and long-term depression in the hippocampus. *Brain Research* **1621** 133–146. (<https://doi.org/10.1016/j.brainres.2014.12.002>)
- Nilsson ME, Vandenberg L, Tivesten Å, Norlén AK, Lagerquist MK, Windahl SH, Börjeson AE, Farman HH, Poutanen M, Benrick A, *et al.* 2015 Measurement of a comprehensive sex steroid profile in rodent serum by high-sensitive gas chromatography-tandem mass spectrometry. *Endocrinology* **156** 2492–2502. (<https://doi.org/10.1210/en.2014-1890>)
- Otto C, Fuchs I, Kauselmann G, Kern H, Zevnik B, Andreasen P, Schwarz G, Altmann H, Klewer M, Schoor M, *et al.* 2009 GPR30 does not mediate estrogenic responses in reproductive organs in mice. *Biology of Reproduction* **80** 34–41. (<https://doi.org/10.1095/biolreprod.108.071175>)
- Pechenino AS & Frick KM 2009 The effects of acute 17beta-estradiol treatment on gene expression in the young female mouse hippocampus. *Neurobiology of Learning and Memory* **91** 315–322. (<https://doi.org/10.1016/j.nlm.2008.09.017>)
- Pompili A, Tomaz C, Arnone B, Tavares MC & Gasbarri A 2010 Working and reference memory across the estrous cycle of rat: a long-term study in gonadally intact females. *Behavioural Brain Research* **213** 10–18. (<https://doi.org/10.1016/j.bbr.2010.04.018>)
- Prange-Kiel J, Jarry H, Schoen M, Kohlmann P, Lohse C, Zhou L & Rune GM 2008 Gonadotropin-releasing hormone regulates spine density via its regulatory role in hippocampal estrogen synthesis. *Journal of Cell Biology* **180** 417–426. (<https://doi.org/10.1083/jcb.200707043>)
- Ruiz de Azua I, Nakajima K, Rossi M, Cui Y, Jou W, Gavrilova O & Wess J 2012 Spinophilin as a novel regulator of M3 muscarinic receptor-mediated insulin release in vitro and in vivo. *FASEB Journal* **26** 4275–4286. (<https://doi.org/10.1096/fj.12-204644>)
- Sheppard PAS, Choleris E & Galea LAM 2019 Structural plasticity of the hippocampus in response to estrogens in female rodents. *Molecular Brain* **12** 22. (<https://doi.org/10.1186/s13041-019-0442-7>)
- Smejkalova T & Woolley CS 2010 Estradiol acutely potentiates hippocampal excitatory synaptic transmission through a presynaptic mechanism. *Journal of Neuroscience* **30** 16137–16148. (<https://doi.org/10.1523/JNEUROSCI.4161-10.2010>)
- Smith CC & McMahon LL 2005 Estrogen-induced increase in the magnitude of long-term potentiation occurs only when the ratio of NMDA transmission to AMPA transmission is increased. *Journal of Neuroscience* **25** 7780–7791. (<https://doi.org/10.1523/JNEUROSCI.0762-05.2005>)
- Srivastava DP & Evans PD 2013 G-protein oestrogen receptor 1: trials and tribulations of a membrane oestrogen receptor. *Journal of Neuroendocrinology* **25** 1219–1230. (<https://doi.org/10.1111/jne.12071>)
- Srivastava DP, Woolfrey KM, Jones KA, Shum CY, Lash LL, Swanson GT & Penzes P 2008 Rapid enhancement of two-step wiring plasticity by estrogen and NMDA receptor activity. *Proceedings of the National Academy of Sciences of the United States of America* **105** 14650–14655. (<https://doi.org/10.1073/pnas.0801581105>)
- Stackman RW, Blasberg ME, Langan CJ & Clark AS 1997 Stability of spatial working memory across the estrous cycle of Long-Evans rats. *Neurobiology of Learning and Memory* **67** 167–171. (<https://doi.org/10.1006/nlme.1996.3753>)
- Tabatadze N, Huang G, May RM, Jain A & Woolley CS 2015 Sex differences in molecular signaling at inhibitory synapses in the hippocampus. *Journal of Neuroscience* **35** 11252–11265. (<https://doi.org/10.1523/JNEUROSCI.1067-15.2015>)
- Taxier LR, Gross KS & Frick KM 2020 Oestradiol as a neuromodulator of learning and memory. *Nature Reviews. Neuroscience* **21** 535–550. (<https://doi.org/10.1038/s41583-020-0362-7>)
- Tetel MJ & Pfaff DW 2010 Contributions of estrogen receptor- α and estrogen receptor- β to the regulation of behavior. *Biochimica et Biophysica Acta* **1800** 1084–1089. (<https://doi.org/10.1016/j.bbagen.2010.01.008>)
- Tian Z, Wang Y, Zhang N, Guo YY, Feng B, Liu SB & Zhao MG 2013 Estrogen receptor GPR30 exerts anxiolytic effects by maintaining the balance between GABAergic and glutamatergic transmission in the basolateral amygdala of ovariectomized mice after stress. *Psychoneuroendocrinology* **38** 2218–2233. (<https://doi.org/10.1016/j.psyneuen.2013.04.011>)
- Toufexis DJ, Myers KM & Davis M 2006 The effect of gonadal hormones and gender on anxiety and emotional learning. *Hormones and Behavior* **50** 539–549. (<https://doi.org/10.1016/j.yhbeh.2006.06.020>)
- Tozzi A, Durante V, Manca P, Di Mauro M, Blasi J, Grassi S, Calabresi P, Kawato S & Pettorossi VE 2019 Bidirectional synaptic plasticity is driven by sex neurosteroids targeting estrogen and androgen receptors in hippocampal CA1 pyramidal neurons. *Frontiers in Cellular Neuroscience* **13** 534. (<https://doi.org/10.3389/fncel.2019.00534>)
- Vallejo D, Codocedo JF & Inestrosa NC 2017 Posttranslational modifications regulate the postsynaptic localization of PSD-95. *Molecular Neurobiology* **54** 1759–1776. (<https://doi.org/10.1007/s12035-016-9745-1>)
- Vierk R, Glassmeier G, Zhou L, Brandt N, Fester L, Dudzinski D, Wilkars W, Bender RA, Lewerenz M, Gloger S, *et al.* 2012 Aromatase inhibition abolishes LTP generation in female but not in male mice. *Journal of Neuroscience* **32** 8116–8126. (<https://doi.org/10.1523/JNEUROSCI.5319-11.2012>)
- Wang C, Dehghani B, Magrizzo IJ, Rick EA, Bonhomme E, Cody DB, Elenich LA, Subramanian S, Murphy SJ, Kelly MJ, *et al.* 2008 GPR30 contributes to estrogen-induced thymic atrophy. *Molecular Endocrinology* **22** 636–648. (<https://doi.org/10.1210/me.2007-0359>)
- Wang W, Le AA, Hou B, Lauterborn JC, Cox CD, Levin ER, Lynch G & Gall CM 2018 Memory-related synaptic plasticity is sexually dimorphic in rodent hippocampus. *Journal of Neuroscience* **38** 7935–7951. (<https://doi.org/10.1523/JNEUROSCI.0801-18.2018>)
- Warren SG, Humphreys AG, Juraska JM & Greenough WT 1995 LTP varies across the estrous cycle: enhanced synaptic plasticity in proestrus rats. *Brain Research* **703** 26–30. ([https://doi.org/10.1016/0006-8993\(95\)01059-9](https://doi.org/10.1016/0006-8993(95)01059-9))
- Warren SG & Juraska JM 1997 Spatial and nonspatial learning across the rat estrous cycle. *Behavioral Neuroscience* **111** 259–266. (<https://doi.org/10.1037/0735-7044.111.2.259>)

Waters EM, Thompson LI, Patel P, Gonzales AD, Ye HZ, Filardo EJ, Clegg DJ, Gorecka J, Akama KT, McEwen BS, *et al.* 2015 G-protein-coupled estrogen receptor 1 is anatomically positioned to modulate synaptic plasticity in the mouse hippocampus. *Journal of Neuroscience* **35** 2384–2397. (<https://doi.org/10.1523/JNEUROSCI.1298-14.2015>)

Woolley CS, Gould E, Frankfurt M & McEwen BS 1990 Naturally-occurring fluctuation in dendritic spine density on adult hippocampal pyramidal neurons. *Journal of Neuroscience* **10** 4035–4039. (<https://doi.org/10.1523/JNEUROSCI.10-12-04035.1990>)

Xu W, Cao J, Zhou Y, Wang L & Zhu G 2018 GPR30 activation improves memory and facilitates DHPG-induced LTD in the hippocampal CA3

of middle-aged mice. *Neurobiology of Learning and Memory* **149** 10–19. (<https://doi.org/10.1016/j.nlm.2018.02.005>)

Yokoi N, Fukata Y, Sekiya A, Murakami T, Kobayashi K & Fukata M 2016 Identification of PSD-95 depalmitoylating enzymes. *Journal of Neuroscience* **36** 6431–6444. (<https://doi.org/10.1523/JNEUROSCI.0419-16.2016>)

Zheng Y, Wu M, Gao T, Meng L, Ding X, Meng Y, Jiao Y, Luo P, He Z, Sun T, *et al.* 2020 GPER-deficient rats exhibit lower serum corticosterone level and increased anxiety-like behavior. *Neural Plasticity* **2020** 8866187. (<https://doi.org/10.1155/2020/8866187/1155>)

Received 25 August 2022

Accepted 3 July 2023

Available online 3 July 2023

Version of Record published 2 August 2023